DANMARKS OG GRØNLANDS GEOLOGISKE UNDERSØGELSE RAPPORT 2010/68

Testing the use of geochemical characteristics of corundum from Greenland as a tool for geographical typing

Per Kalvig og Dirk Frei

GEOLOGICAL SURVEY OF DENMARK AND GREENLAND
MINISTRY OF CLIMATE AND ENERGY

G E U S

DANMARKS OG GRØNLANDS GEOLOGISKE UNDERSØGELSE RAPPORT 2010/68

Testing the use of geochemical characteristics of corundum from Greenland as a tool for geographical typing

Per Kalvig og Dirk Frei

GEOLOGICAL SURVEY OF DENMARK AND GREENLAND
MINISTRY OF CLIMATE AND ENERGY

GEUS

Content

Abstract

In order to test the use of geochemical characteristics as a tool for geographical typing of corundum, a total of 16 corundum samples representing the corundum localities of Fiskenæsset, Nuuk, Maniitsoq, and Tasiilaq, as well as one from Macedonia, have been analyzed by means of LA-ICP-MS techniques. All samples were picked from corundum specimens available at GEUS and BMP.

The survey revealed that the selected samples from Greenland show a relatively homogeneous chemistry and limited intra sample variation. The samples plot within relatively continuous fields in chemical variation diagrams and in the discrimination diagrams commonly used to characterise gem corundum. There is an overlap between individual samples that at the present state of knowledge does not allow unequivocal identification of sample provenance based on chemistry alone.

Three samples (sample 497383 from Top 670, Fiskenæsset; sample 319411 from Tasiilaq and sample 497399 from Macedonia) show distinctive chemical signatures related to extreme enrichment or depletion of certain trace elements. However, the samples from Top 670 show that even within a single outcrop extreme geochemical variation can occur urging some caution concerning geographic typing based on corundum geochemistry alone.

In order to utilize the geochemical record in Greenlandic corundum as a tool for geographical typing, additional work will be required. This should encompass: (i) Detailed studies on intra-grain, intra-sample and intra-locality chemical variability of corundum; (ii) Crystallographic and optical work, as supplementary data to the geochemical characteristics of corundum; (iii) A comprehensive corundum database for Greenlandic and non-Greenlandic samples for comparison purposes; and (iv) Geographic discrimination employing a multivariate statistical approach, such as pattern recognition with principal component analysis (PCA).

1. Introduction

The gemstone industry in Greenland has for many years comprised only a few enthusiastic individuals, cutting and polishing domestic stones (f. ex. agate, amazonite, garnet, ‘nuumiit’, tugtupite, red corundum (ruby)) mainly for sale among tourists visiting the townships in the southern part of West Greenland. In the late sixties red corundum was discovered in the Fiskenæsset region in relation to altered ultrabasic rocks, and later corundum occurrences have been discovered at various places in both West and East Greenland. The Mining Act was amended in 2009; the amended act allows small scale operations by individuals living in Greenland.

On this background the Bureau of Minerals and Petroleum (BMP) and the Geological Survey of Denmark and Greenland (GEUS) decided in September 2009 to enter into a mutual research project on geochemical characterisation of corundum minerals collected from localities in Greenland. The successful technology being looked for should include a non-destructive method enabling the BMP and other Greenlandic authorities to prove or disprove a Greenlandic provenance on internationally traded rubies.

It was agreed to undertake a geochemical characterization by means of Laser Ablation-Inductively Coupled Plasma Mass Spectroscopy (LA-ICP MS) and supplementary investigations of some of the corundum crystals by Scanning Electron Microscope (SEM). This report conveys the results of the research.

Chemically considered, corundum is pure alumina (Al_2O_3); however chemical impurities are frequently present in large amounts, up to 10%; in particular corundum contains iron oxide, silica and traces of chromium oxide. The chemical composition of a corundum stone has influence on the character of the stone in terms of colour, transparency, and aesthetical value. The chemical composition of transparent red corundum, the so-called “oriental ruby” and of a blue corundum or “oriental sapphire”, include small amounts of iron oxide and silica (total ~2 %) and trace amounts of chromium oxide. The colours vary in tone from light and pale to dark and intense. This study applies the term corundum without any pre-fix indicating the quality of the stone.

The appearance of corundum in terms of colour and transparency varies a great deal. Most frequently the mineral is cloudy and opaque and only a small proportion is clear and transparent and thereby valuable. The cloudy and opaque type is normally not considered by the gem industry, but has been included in this study, since no distinction has been made between gem quality stones and stones of no commercial value.

Analytical data and photographs are enclosed in Appendix.

2. Corundum localities in Greenland

The first red corundum minerals were discovered on Arsuk Storø by Giesecke in 1806 (though disputed by Bøggild (1953)), and in the Fiskenæsset area in 1816, also by Giesecke (Giesecke 1816). Additionally, corundum has been reported from Uiffaq, the Godhavn District (Bøggild 1953).

The main exploration for red corundum has taken place after the discovery of red corundum on the 'Rubin Ø' (Ruby Island), south of the township Fiskenæsset, SW Greenland, in 1966 by the Geological Survey of Greenland (GGU). Subsequently, exploration for corundum has been undertaken by Platinomino A/S in the 1970's and 1980'ies, and by Valhall Mining Ltd in 1995. Since 2004, True North Gems Inc. has undertaken extensive corundum exploration in the Fiskenæsset area, and about thirty localities of red and pink corundum have been recorded. The geology of the Fiskenæsset area has been presented in numerous papers, e.g. Kalsbeek & Garde (1989); the Fiskenæsset complex is described by Myers (1985) and the chromites of the complex by Ghisler (1976). Appel (1995), Herd (1973) and Herd *et al.* (1969) provide information on the corundum mineralisation. Recently, Weston (2009) reports the exploration results achieved by True North Gems Inc. on the red corundum of the Fiskenæsset region.

Scattered corundum localities have been found by GEUS – and local individuals – at several places in Greenland:

Disko Bary area (Pedersen 1978 and Pedersen 1981)
Nuuk area, West Greenland
Maniitsoq, West Greenland
Tasiilaq, East Greenland

3. Samples and sample description

It has been a precondition of the project that samples included have been chosen based on availability and geographical diversity rather than their potential gem quality. Thus 11 samples from the Fiskenæsset area, one sample from Maniitsoq, three samples from the Nuuk region and two samples from East Greenland have been included; additionally, one sample from Macedonia, as the only available sample from outside Greenland has been included. The actual sample co-ordinates of some of the samples are unknown; due to the scope and nature of this investigation, we have disregarded this fact.

Table 1: *Corundum samples included in the geochemical survey. Macro description of the colours codes of the samples is undertaken in accordance with Kornerup & Wanscher (1974).*

Locality	**Sample no.**	**Colour /code**
Fiskenæsset region		
Annertusoq	497394	Greyish magenta /13D7
Annertusoq	78667	Redish lilac/ 14B4
Annertusoq	476321	Greyish magenta/ 13D3
Aappaluttoq	497395	Greyish magenta / 14F6
Beer Mnt.	1258 = 497391	Greyish ruby/ 12D6
Bjørnesund NW	513743	Greyish magenta / 13D5
Rubin Ø	497393	Greyish ruby / 12C7
Siggartartulik	497392	Greyish ruby/ 12E7
Top 670	497375	Greyish magenta /13E6
Top 670	497383	Reddish lilac / 14B3
Top 670	497386	Greyish ruby – ruby red / 12D7
Maniitsoq region		
Maniitsoq	289933	Greyish magenta / 13E6
Nuuk region		
Nuuk – Storø	497396	Greyish magenta / 14E4
Kapisillit – blue korundum	224779	Turquoise grey / 24F2
East Greenland		
Tasiilaq	319411	Bluish grey / 20E2
Nugtivit (Ujarassiorit 2009)	497397	Pale violet / 15A3
International		
Macedonia	497399	Greyish magenta / 13D4

Macro description of the colours codes of the samples is undertaken in accordance with Kornerup & Wanscher (1974).

All scale subdivisions used on the macro-photographs are in millimetres.

3.1 Fiskenæsset / Qeqertarsuatsiaq

Annertusoq (Angnertusoq old spelling)

Upper Annertusoq (63 00' 42.7''N/ 50 25' 52.6'' W)

Lower Annertusoq (63 00' 25.0''N/ 50 28' 43.2'' W)

Annertusoq mountain lies at the eastern end of Kigutilik bay about 13 km SE of Fiskeneasset township.

The Lower Annertusoq corundum-bearing rocks are found within a moderately exposed lens (26 m x 2 m) situated along the contact between a chromite-layered anorthosite and a pyribolite/amphibolite horizon, and several corundum-bearing parageneses have been reported (Herd *et al*. 1969).

The Upper Annertusoq locality lies on the south-east side of Annertusoq mountain at an altitude of 390 m in a layer within the same anorthosite horizon as that of Lower Annertusoq (Herd *et al* 1969).

According to Appel (1995), both localities belong to the gedrite-type, composed by gedrite, corundum, sapphirine, phlogopite, +/- cordierite, +/- spinel. Corundum is red and generally medium grained and fractured.

Three samples from Annertusoq are included in this survey (no.'s: 487394, 78667, and 476321); no details whether they are sampled at Lower- or Upper Annertusoq. Brief macro-descriptions of the involved samples from Annertusoq are provided with the figures 1 to 5.

Figure 1. *Sample 78667-Annertusoq: Amphibolite with euhedral redish lilac corundum crystals (~35 x 12 mm); not translucent.*

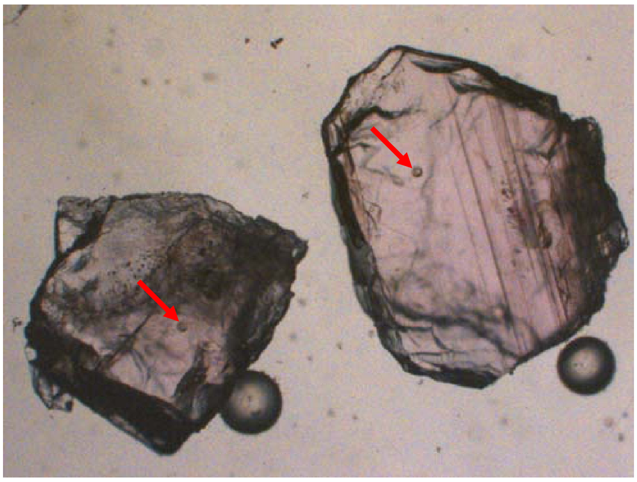

Figure 2. *Photomicrograph of corundum crystals separated from sample 78667 (Annertusoq). The ablation craters (indicated by arrows) caused by the laser during LA-ICP-MS measurements are 45 µm in diameter and barely visible to the naked eye.*

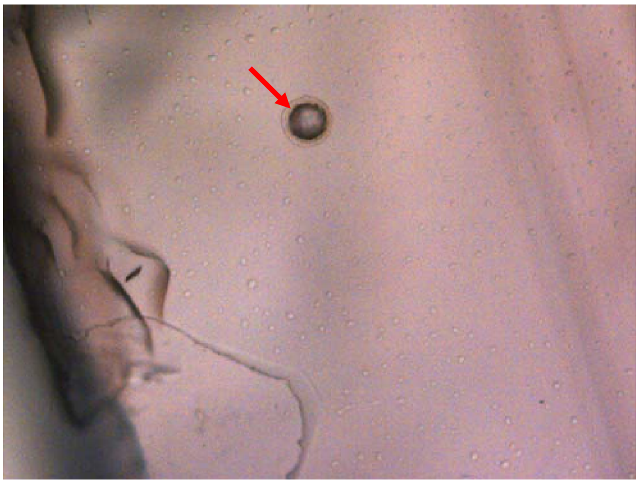

Figure 3. *Photomicrograph showing details of an ablation crater (45 µm in diameter) in a corundum crystal separated from sample 7866 (Annertusoq). Note also that corundum from sample 78667 shows frequent mineral- and melt inclusions, but the high spatial resolution of the laser ablation analysis allows analysis of inclusion-free areas.*

Figure 4. *Sample 476321 - Annertusoq: Aggregate of greyish magenta corundum in ultramafic rock; occurs with rutile phenoblasts.*

Figure 5. *Sample 497394- Annertusoq: Greyish magenta coloured corundum in a matrix of green pargasite, phlogopite and plagioclase; corundum crystals elongated parallel to the foliation of the rock; crystals from 1- 10 mm.*

Siggartartulik *(62 59’ 05.3’’N/ 50 25’ 37.0’’ W)*

Appel (1995) classifies the Siggartartulik corundum showing as belonging to his pargasite type. The typical paragenesis of this type consists of pargasite, red corundum, sapphirine, +/- plagioclase, +/- cordierite, +/- spinel, +/- phlogopite. The grains of red corundum are mostly fractured and up to 20 mm long; the corundum crystals are often rimmed by narrow zones of spinel and sapphirine. According to Appel (1995), the Siggartartulik showing is the largest showing of red corundum. Samples are shown in figure 6.

Figure 6. *Sample 497392 - Siggartarlulik: Greyish ruby coloured corundum gravel material sampled by Ole V. Petersen, 1975. The colour variegates from greyish magenta to ruby red; the corundum minerals are up to 5 mm in size; the transparency is fairly good.*

Aappaluttoq (Aappaluttoq - old spelling) ***I*** *(63 00’ 39.2’’N/ 50 19’ 10.9’’ W)*

At Aappaluttoq, gem quality corundum has been known for years, and in 2007-2008 the zone has been explored further by True North Gems Ltd.; the red and pinkish corundum are found in a paragenesis of sapphirine-gedrite-phlogopite-pargasite. Some of the most valuable gem corundum of the Fiskenæsset area stems from this locality. The sample is shown in figure 7.

Figure 7. *Sample 497395 - Aappaluttoq: The sample of corundum in a pargasite matrix; the crystals are 12 mm, subhedral, mainly and greyish magenta colours dominate.*

.

Beer Mountain *(63 08' 25''N/ 49 34' 58'' W)*

Scattered crystals of red corundum are found in a gabbroic layer within the anorthosite complex; the corundum is rimmed with plagioclase and mica in a hornblende matrix (Appel, 1995). The red corundum crystals are reported to be up to 20 cm long, but only fractured crystals have been seen; variegated deep red to pink colours. Appel (1995) classifies this occurrence as belonging to the hornblendite type. The sample is shown in figure 8.

***Figure 8.** Sample no: 1258 = 497391- Beer Mountain: (sampled 14/8 – 1970; PA locality 14) Hornblende anorthosite with greyish ruby coloured corundum; up to 25 mm sub-euhedral crystals.*

Bjørnesund NW *(63.1268 N/ 49.7408 W)*

Red corundum has been observed in a 1.6 km long, semi-continuous ultramafic schist rich in phlogopite; kornerupine occurs but is not very common, and pargasite has not been observed. The thickness of this horizon varies from few centimetres to about two metres. The colour of the corundum minerals variegates between light pink to pink; the crystals are in general not transparent. The sample is shown in figure 9.

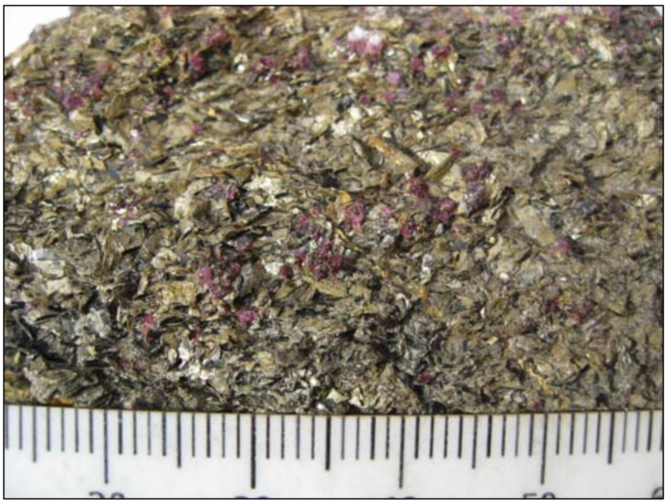

***Figure 9.** Sample 513743 – Bjørnesund NW: Ultramafic rock dominated by phlogopite with disseminated corundum (< 1mm); the dominant colour of the corun-*

dum is greyish magenta; some few more reddish.

Rubin Ø (Ruby Island), **Tasiusarsuaq** *(63 02' 10.6''N/ 50 17'13.6'' W)*

The corundum bearing rocks on Rubin Ø in Tasiussaa bay at the head of Tassiussarssuaq fjord occur in an ultramafic layer with anorthosite to the west and amphibolite to the east; commonly, the red corundum is associated with sapphirine and phlogopite (Herd *et al* 1969). The sample is shown in figure 10.

Figure 10. *Sample 497393 – Rubin Ø: Ultramafic rock dominated by phlogopite; red corundum occurs as disseminated, subhedral crystals (< 1mm); most of the crystals are transparent and clear red.*

Top 670 *(63.1279 N/ 50.2897 W)*

Locality 09PKa98: Red corundum is observed in a 10 x 2 m wide lens-shaped ultramafic rock dominated by phologopite, kornerupine, gedrite and very little pargasite. The red corundum is typically < 1 mm and pinkish red in colour. The sample is shown in figure11.

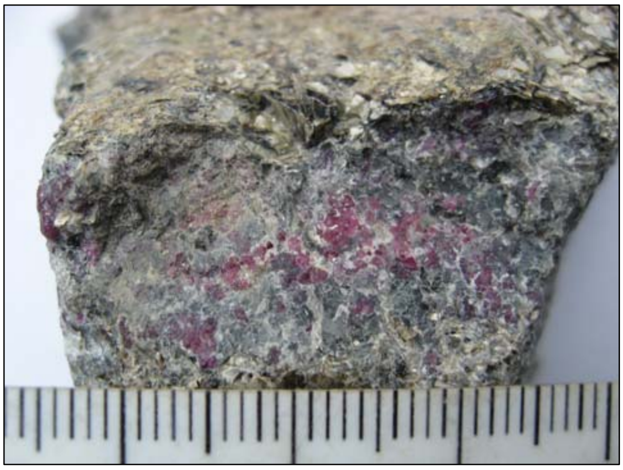

Figure 11. *Sample 497375 – Top 670: Plagioclase, phlogopite, amphibole-rich ultramafic rock with disseminated greyish magenta coloured, subhedral corundum; crystals in general < 1 mm, but some up to 3 mm.*

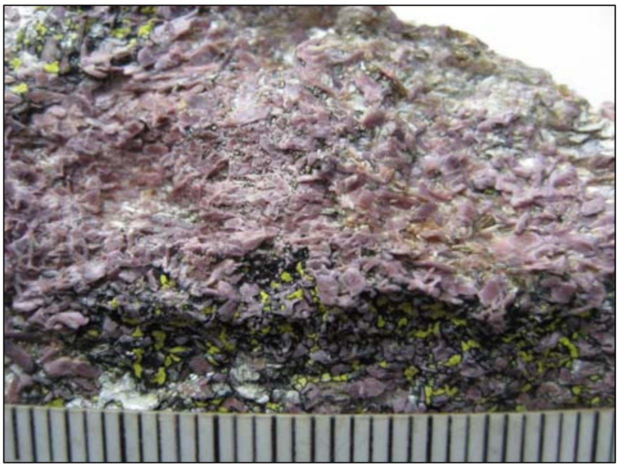

Figure 12. *Sample 497383 – Top 670: Mica-rich ultramafic rock with reddish lilac corundum crystals; the corundum occurs mainly in aggregate composed by 0.5-2 mm individual euhedral grains; the grains are cloudy.*

Figure 13. *Sample 497386 – Top 670: Greyish ruby – ruby red coloured corundum in phlogopite-rich ultramafic rock; corundum forms aggregates composed by <
1 mm subhedral crystals.*

3.2 Nuuk district

Figure 15. *Sample 224779 – Nuuk district: Sample from Kapisillit. Two c. 15 mm corundum crystals both dominantly of turquoise grey colour.*

Figure 16. *Sample 497396 – Nuuk district: Sample from Nuuk Storø: Two crystals corundum of variegated greyish magenta coloured corundum; sample is rather opaque.*

3.3 Maniitsoq district

The actual locality of this sample is not known, but the sample is assumed to stem from a locality c. 2 km NW of Maniittsoq, where a sapphirine-bearing hornblendite has been described by Herd et al (1969).

Figure 17. *Sample 289933 - Maniitsoq: Small samples of corundum; variegated brownish red colour; cloudy appearance.*

3.4 East Greenland

No information is available about the geology at the sample locations of the samples gathered in East Greenland. Sample 497397, achieved the first prize in the Ujarassorit 2009, is found near Nugtivit, South of Tasiilaq. The sample is shown in figures 18 and 19.

Figure 18. *Sample 497397- Nugtivit: Pale violet corundum in a matrix of green amphibole (pargasite?); crystals > 12 mm.*

Figure 19. *Sample 319411- Tasiilaq: Weathered bluish grey corundum aggregate.*

3.5 Samples from outside Greenland

Macedonia

One sample from Macedonia has been included for reference. The sample was kindly provided by M. Ghisler.

Figure 20. *Sample no. 497399 - Macedonia: Greyish magenta coloured corundum aggregate – c. 22 mm long; not transparent.*

3. Sample preparation and analytical techniques

3.1 Sample preparation

After visual inspection, a small fragment of corundum was chipped of each sample using a geological hammer. The resulting chips were further broken into small pieces using the geological hammer, followed by very gentle disaggregation using a pestle and mortar, avoiding grinding action. A split of each sample was retained and handed over to the RD for further study. Under a binocular microscope, two to five corundum crystals were subsequently hand-picked, from each sample; these grains were selected according to optical clearness. Following hand-picking, the samples were immersed in water and cleaned ultrasonically to remove and disperse any fine material that might have been adhering to grain surfaces.

For trace element determinations, crystals were mounted on adhesive tape, cast in 1-inch diameter circular epoxy mounts, ground to approximately 80% of the original crystal thickness, and polished using 1 µm diamond polishing paste. In order to select inclusion- and crack-free areas for analysis, all grains were studied under a binocular and polarizing microscope prior to analysis. All crystals were again inspected by binocular- and polarizing microscope after analysis and photographed for documentation (see attached DVD: corundum photomicrographs.ppt).

3.2 In-situ trace element analysis by LA-SF-ICP-MS

The corundum crystals utilised in this reconnaissance study have been analysed for their elemental concentrations of Mg, Si, Ti, V, Cr, Fe, Ga, and Ge at GEUS using laser ablation – high resolution – magnetic sectorfield - inductively coupled plasma – mass spectrometry (LA-SF-ICP-MS). This selected range of elements has been chosen because previous corundum provenance studies have demonstrated that they have the highest discriminative power (e.g., Sutherland *et al.* 1998, Guillong and Günther 2001, Limtrakun *et al.* 2001, Peucat *et al.* 2007, Sutherland and Abduriyim 2009) and are therefore especially suited for a reconnaissance study.

The instrumental set-up consists of a NewWave Research/Merchantek UP213 laser ablation system equipped with a frequency quintupled ND-YAG laser emitting at a wavelength of 213 nm, coupled to an Element2 (ThermoFinnigan, Bremen) single-collector double focusing magnetic sectorfield ICPMS in reversed Nier-Johnson geometry equipped with a fast fieldregulator for increased scanning speed (see Liebscher *et al*. 2007 for a detailed description of the set-up used in the GEUS LA-SF-ICP-MS facility).

The laser was operated at a repetition rate of 10 Hz and a nominal energy output of 75 %, corresponding to a laser fluency of10 J cm^{-2}. All data were acquired with a single spot analysis on individual corundum grains using a beam diameter of 45 µm. Samples and standards were held in a dedicated low volume ablation cell that enhances signal stability and allows rapid flush-out of residual material after ablation (Frei and Gerdes 2009). Helium was used to flush the sample cell and was mixed downstream with the Ar sample gas of the masspectrometer. The washout time for this configuration is approximately 15 seconds. The sample mount was rigorously cleaned to remove surface contaminations before introduction into the sample cell.

The total acquisition time for each analysis was 60 s with the first 30 s used to measure the gas blank. The mass spectrometer was tuned to give large, stable signals for the ^{49}Ti and ^{69}Ga peaks, low background count rates (typically around zero counts per second for the REE) and low oxide production rates ($^{232}Th^{16}O/^{232}Th$ generally below 0.1 %). All measurements were performed in low resolution mode using electrostatic scanning (E-scan). All data were acquired in time-resolved analysis (TRA) mode using peak jumping with one sample per peak with a sampling time of 10 ms for each isotope. The following masses were measured and ratio'ed to ^{27}Al for internal standardization using the stoichiometric concentration of Al: ^{25}Mg, ^{27}Al (internal standard), ^{49}Ti, ^{51}V, ^{52}Cr, ^{57}Fe, ^{69}Ga, and ^{72}Ge. For calibration and quality control, the NIST SRM 612 and 614 glass standards were applied for all analyses. In a typical analysis sequence two standards are analysed initially, followed by five unknown samples, again two standards, and so on. Data reduction and concentration calculation was performed using the GLITTER software package using the calibration values of Pearce et al. (1997). The results for the NIST SRM 614 glass standard that was analysed routinely for quality control purposes are consistently within 2 s of published concentrations. Under these conditions, the detection limits are, except for Mg, Si and Fe, in the ppb range (Appendix A) and the analytical uncertainty is generally **<10%** relative (at 1 sigma level).

4. Results and discussion

About two to five individual crystals from each of the 18 samples investigated have been analysed by LA-SF-ICP-MS, resulting in a total of 65 individual trace element analyses. All results obtained are reported here, together with the minimum detection limit and the analytical uncertainty (Appendix A).

Corundum usually consists of more than 98% of Al_2O_3 and can contain various trace elements. However, the highest trace element contents are usually observed for Mg, Fe, Ti, V and Cr. Other elements, such as Ga and Ge are also present in corundum, but in lesser amounts. The colouring of corundum is related to the incorporation of trace amounts of Cr, Fe and Ti: Cr causes the red colour of rubies, while Fe and Ti are responsible for the blue colour of sapphires.

The use of trace elements incorporated in corundum for provenance characterisation has already been demonstrated by a number of studies (e.g., Calligaro *et al.* 1998, 1999, Sutherland *et al.* 1998, Guillong and Günther 2001, Limtrakun *et al.* 2001, Peucat *et al.* 2007, Sutherland and Abduriyim 2009). Most significantly, it has been shown that differences in the composition of trace elements exist between magmatic and metamorphic corundum (Sutherland et al. 1998, Limtrakun et al. 2001, Saminpanya et al. 2003, Sutherland and Abduriyim 2009). Sutherland et al. (1998) suggested that metamorphic suites are characterized by high Cr and low Ga contents with Cr_2O_3/Ga_2O_3 ratios above 3, whereas magmatic suites exhibit high Ga and low Cr contents with Cr_2O_3/Ga_2O_3 ratios below 1. Based on a study of the trace element concentrations in blue sapphires (i.e., Fe+Ti dominant corundum), Peucat *et al.* (2007) demonstrated that the Ga/Mg ratio combined with the Fe concentration is an efficient geochemical tool for discriminating between metamorphic and magmatic blue sapphires. This work was further elucidated by a study of Sutherland and Abduriyim (2009) on the provenance of blue sapphires from New South Wales, Australia. They concluded that the Cr/Ga and Fe/Ti ratios are powerful parameters in discriminating between metamorphic and magmatic blue sapphires (Figure 25). In the following, we will describe the trace element variations observed in the corundum crystal investigated in this study and discuss the results using the discrimination schemes of Peucat et al. (2007) and Sutherland and Abduriyim (2009).

The variation of the elements responsible for the colouring of corundum Fe and Ti (blue colour), and Cr (red colour), are shown in Figure 21; colour codes for comparisons are given in Table 1. The observed variations within each sample are relatively small. However, there is considerable overlap between most of the investigated samples. Furthermore, the majority of analyses plot in a more or less continuous field defined by a limited variation of Fe + Ti (ranging from around ~1,000 to ~5,000 ppm, with a median of ~1,600 ppm) and a somewhat larger variation of Cr (ranging from around ~300 to ~11,000 ppm, with a median of ~3,000 ppm) concentrations. The larger variation in Cr contents most likely reflects the variation in red colouring of the investigated crystals. The only blue corundum crystals analysed in this study, from sample 224779 (Kapisillit), show, as expected, relatively low Cr contents. However, their Fe + Ti contents are not elevated and they plot adjacent to red-coloured crystals (e.g., samples 78667 and 497375), suggesting that their blue colour is not entirely controlled by absolute Fe, Ti and Cr concentrations. The variation of Fe, Ti and Cr are plotted as a function of Mg concentration in figure 21.

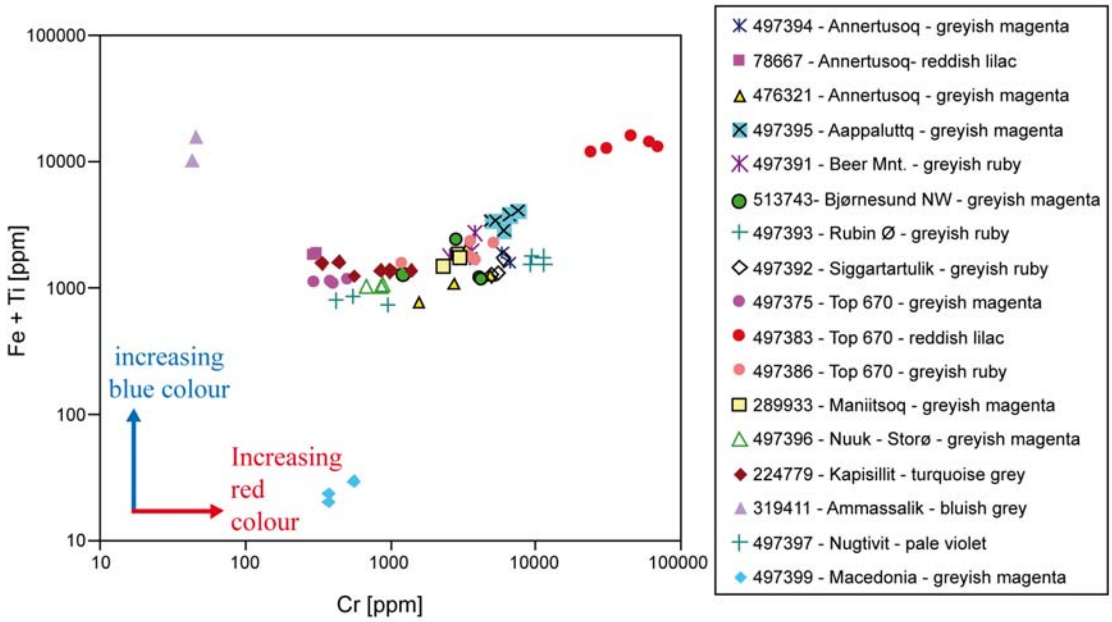

Figure 21. *Fe + Ti vs. Cr diagram for corundum crystals investigated in this study. Vectors shown indicate colouring of corundum as a function of trace element content. Actual colours of corundum crystals shown in legend.*

The most striking feature of Figure 21 is that corundum from three samples plot outside the relatively continuous field defined by the majority of analyses: sample 319411 (Ammassalik) is characterised by high Fe+Ti (mainly due to Fe contents around ~10,000 ppm) and low Cr contents (around ~40 ppm; the lowest observed Cr contents of all investigated samples); sample 497383 (Fiskenæsset Top 670) is characterised by high Fe+Ti (again mainly due to Fe contents around ~10,000 ppm) and high Cr contents (around 10,000 ppm/1 wt-%

ppm; the highest observed Cr contents of all investigated samples); and sample 497399 from Macedonia, which is characterised by low Fe+Ti (around ~20-30 ppm, the lowest observed Fe and Ti contents of all investigated samples) and moderately low Cr contents (~370 ppm).

The continuous variation in chemistry for the majority of the investigated corundum crystals is also observed in figure 22, where the colouring elements Fe (figure 22a), Ti (figure22b), and Cr (figure 22c) are plotted as a function of Mg concentration. Two populations can be identified for both Ti vs Mg and Cr vs Mg; however, the clustering is correlated with neither the geographical distributions nor the colour codes.

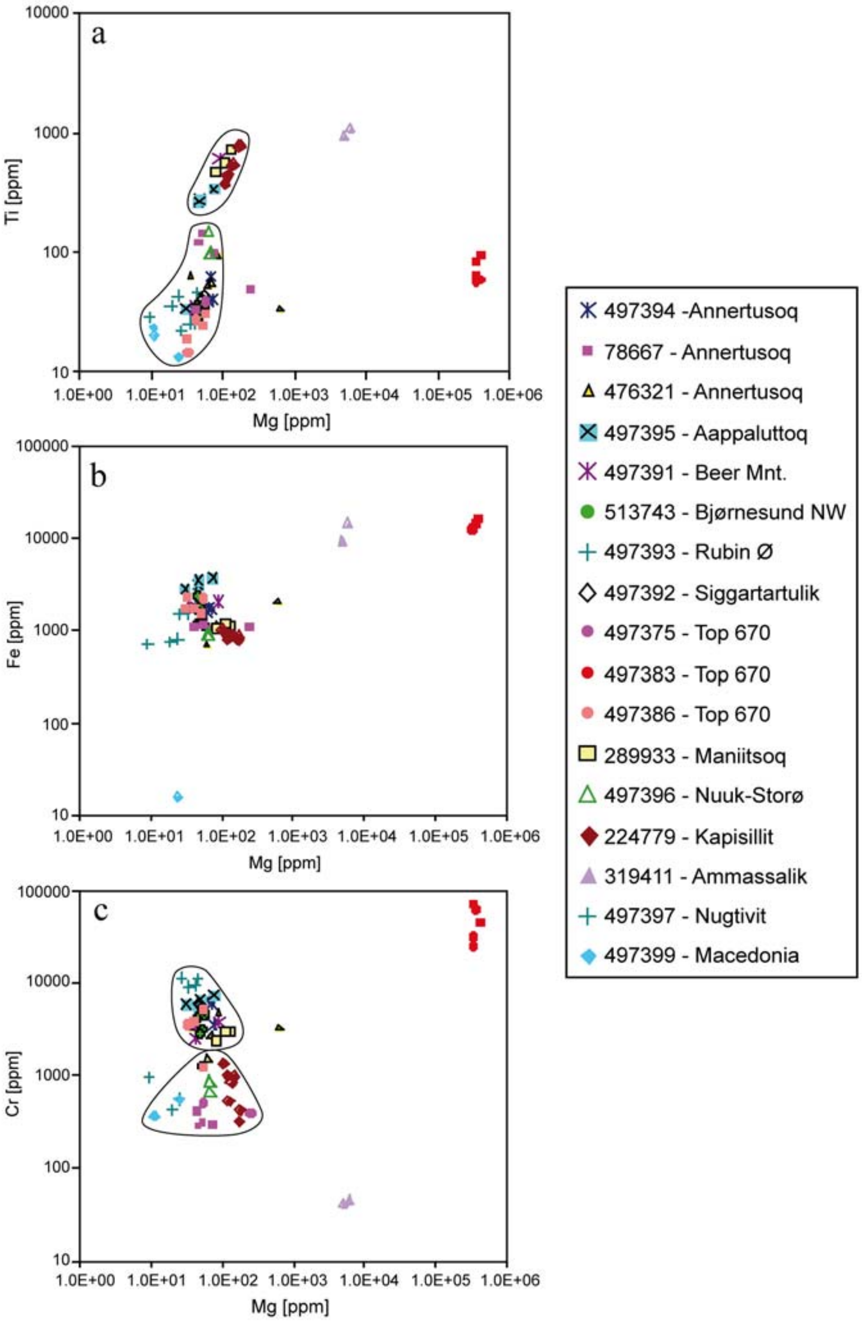

Figure 22. *Fe (a), Ti (b), and Cr (c) vs. Mg diagram for corundum crystals investigated in this study.*

For the majority of the analysed crystals, the Mg content shows a limited intra-sample variation. However, there is considerable overlap between most of the investigated samples. Within the continuous field, the overall variation in Mg contents is from ~10 to ~150 ppm. However, samples 319411 (Ammassalik) and 497383 (Fiskenæsset Top 670) show drastically higher Mg concentrations (~5,000 ppm in sample 319411 and >300,000 ppm / 3 wt -% in sample 497383). The very high concentrations observed for Mg, Fe, and Cr in sample 497383 (partly orders of magnitude higher than expected for corundum) are even more surprising given that corundum investigated in two other samples from the same locality (samples 497375 and 497386) show the elemental trends observed for the majority of crystals studied here. This finding suggests that presumably very local (i.e., on a decimetre scale) chemical exchange processes between ultramafic and aluminous lithologies can lead to extreme chemical variations on an outcrop scale.

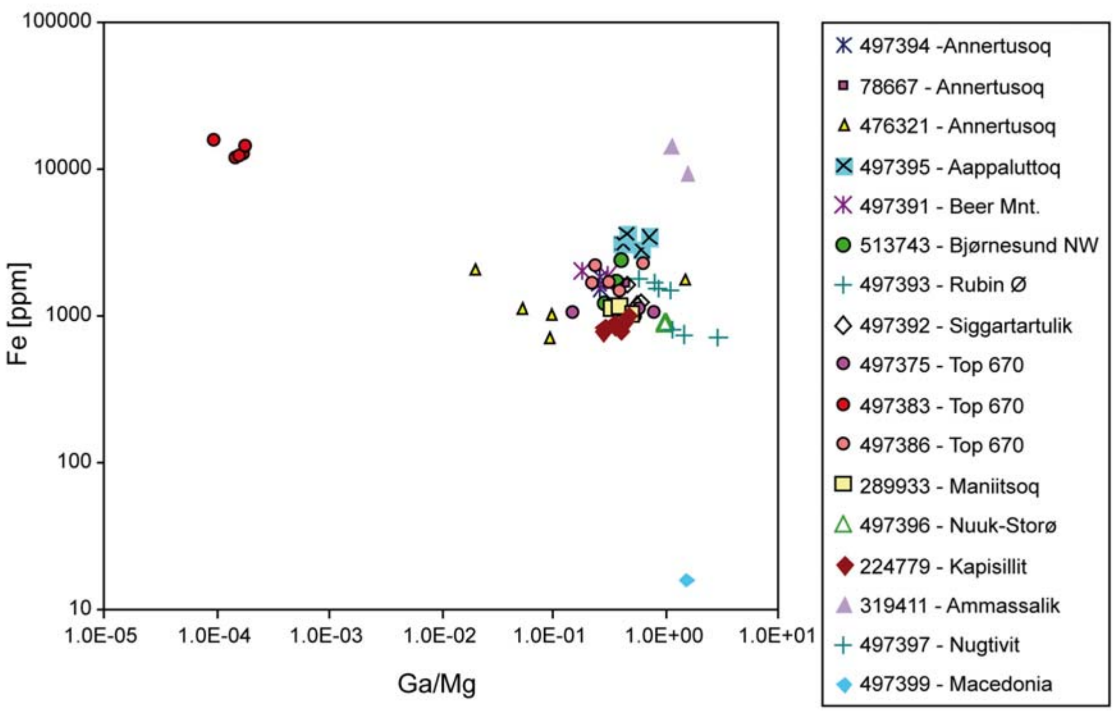

Figure 23. *Fe vs. Ga/Mg diagram for corundum crystals investigated in this study.*

In order to further assess if the geochemical signatures of the investigated Greenlandic corundum crystals can be separated into specific groups, we have plotted the results in the trace element variation diagrams that are commonly used to characterise gem corundum, i.e., the Fe vs. Ga/Mg (figure 23 and 24), Cr/Ga vs. Fe/Ti (figure 25) and Fe/Mg vs. Ga/Mg (figure 26) diagrams (e.g., Sutherland *et al.* 1998, Peucat *et al.* 2001, Sutherland and Abduriyim 2009).

These diagrams are based on the analysis of blue sapphires and might therefore only have limited applicability to the predominantly red corundum investigated in this study. However, we would like to emphasise that the crystals investigated in this study (with the exception of the very Fe-rich sample 497383) have Fe contents that are very similar to those in the blue sapphires used by Sutherland et al. (1998), Peucat et al. (2007) and Sutherland and Abduriyim (2009), and that the application of this diagrams to the Greenlandic red corundum investigated can therefore be considered warranted.

In the Fe vs. Ga/Mg diagram (figure 24), the dataset shows essentially the same features already observed for their Mg, Fe, Ti and Cr distribution. The majority of the data plot in a more or less homogeneous field and show considerable overlap. Again, samples 319411, 497383 and 497399 are plotting in clearly separated fields, reflecting their distinctive Fe and Mg chemistry. In order to better visualise the majority of the data and to compare with the compositional fields indicative for metamorphic blue sapphire (MBS) and magmatic blue sapphire proposed by Peucat *et al.* (2001), we have replotted the dataset in a Fe vs. Ga/Mg diagram with an expanded x-axis in figure 24.

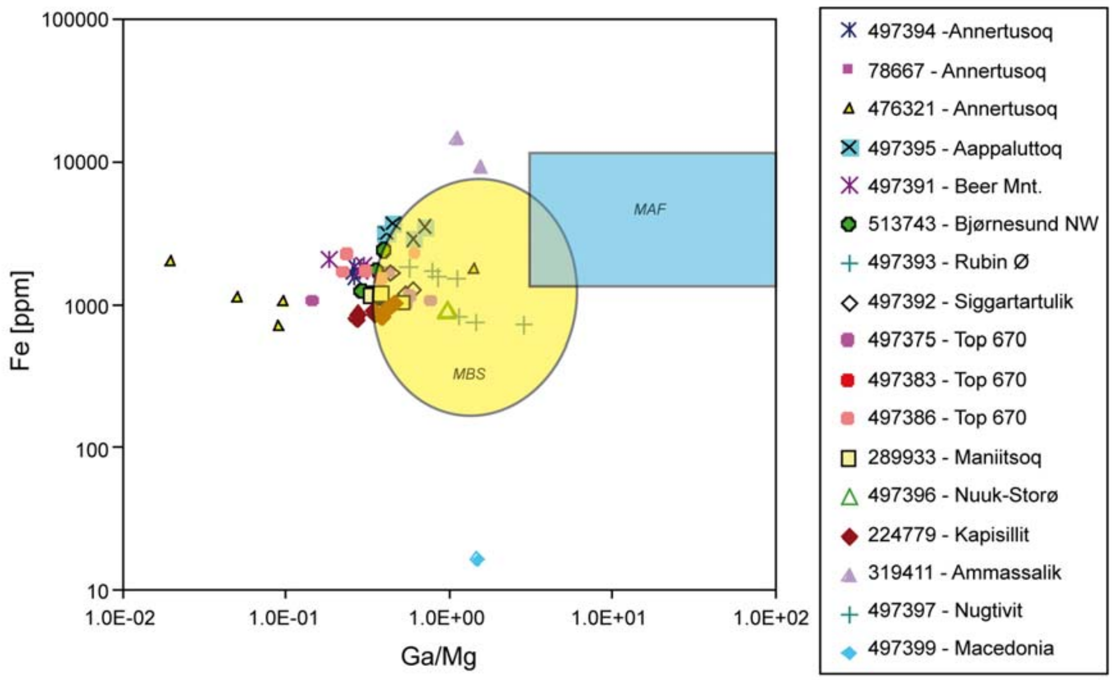

Figure 24. *Fe vs. Ga/Mg diagram with expanded x-axis for corundum crystals investigated in this study. Also shown are fields typical for metamorphic blue sapphire (MBS) and magmatic blue sapphire (MAF), after Peucat et al.(2007).*

Clearly, none of the Greenlandic corundum plot in the field indicative for magmatic blue sapphire. In contrast, the field defined by the Greenlandic red corundum shows a clear overlap with the field indicative for metamorphic blue sapphire, although a significant part is displaced to lower Ga/Mg values. This displacement is caused by significantly higher Mg contents in the Greenlandic red corundum compared to the sapphires studied by Peucat *et al.* (2001) and might reflect the close association of Greenlandic red corundum with Mg-rich ultramafic lithologies. Again, samples 319411 (Ammassalik) and 497399 (Macedonia) plot in very distinctive fields towards relatively high Ga/Mg ratios. In sample 319411, the high Ga/Mg ratio is caused by unusually high Ga concentrations (~7,000 ppm compared to a median of 32 ppm for all samples). In contrast, in sample 497399 the high Ga/Mg ratio is caused by very low Mg concentrations (~10 ppm compared to a median of 55 ppm for all samples).

The unusal Ga-rich nature of sample 319411 is also depicted in the Cr/Ga vs Fe/Ti diagram (figure 25); due to the very high Ga contents, the corundum crystals from sample 319411 plot at low Cr/Ga ratios in the field indicative for magmatic corundum.

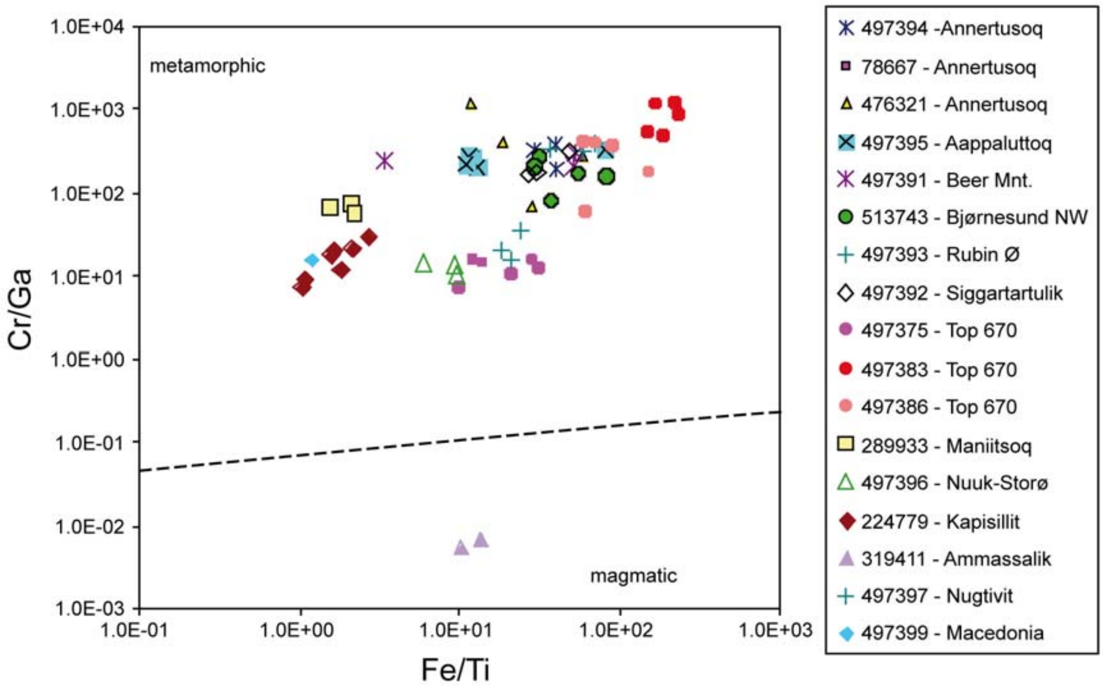

Figure 25. *Cr/Ga vs. Fe/Ti diagram for corundum crystals investigated in this study. The fields indicative for metamorphic blue sapphire and magmatic blue sapphire (following Sutherland and Abduriyim 2009) are separated by the stippled line.*

All other samples, including the in other ways deviating samples 497383 (Top 670, Fiskenæsset) and 497399 (Macedonia) constitute a relatively homogeneous group in the field indicative for metamorphic corundum. Although some samples plot in relatively confined and separate fields (samples 497383 and 289933) there is considerable overlap between most of the investigated samples. Overall, there appears to be a weak positive correlation between Cr/Ga and Fe/Ti ratios.

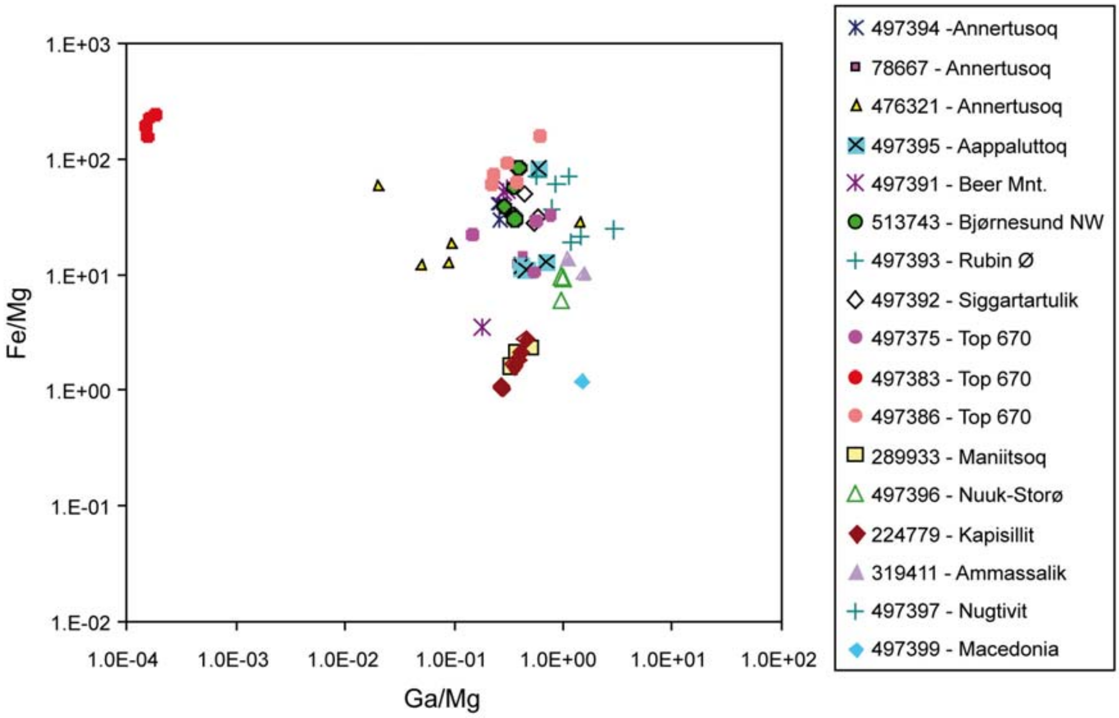

Figure 26. *Fe/Mg vs. Ga/Mg diagram for corundum crystals investigated in this study.*

In the Fe/Mg vs. Ga/Mg diagram (figure 26) all samples (except the extremely Mg-rich sample 497383 from Top 670, Fiskenæsset) plot in a relatively narrow field and do not show any apparent correlations. Most strikingly, although most of the samples show no large-scale intra-sample variations, there is a significant degree of overlap between individual samples that does not allow unequivocal separation of individual samples.

In a previous study, the laboratory of the Gemmological Institute of America in Bangkok investigated the trace element composition of corundum from Aappaluttoq, Fiskenæsset region, Greenland, provided by John L. Emmeret (JLE Associates, Brush Prairie, WA) and samples originating from True North Gems Inc. (unpublished report by Thirangoon). In total, 25 corundum crystals were analysed. The exact sample numbers or localities of the samples are not provided by Thirangoon; however, it can be assumed that the individual crystals are possibly derived from a number of different samples taken at different localities at Aappaluttoq. Hence the data reported by Thirangoon most likely demonstrate the variation in trace element concentrations that can be expected for corundum from a rather restricted, local area.

In the following, we will compare the trace element variations obtained for corundum crystals in this study that are derived from a wide range of localities in Greenland, with those obtained for Aappaluttoq by Thirangoon.

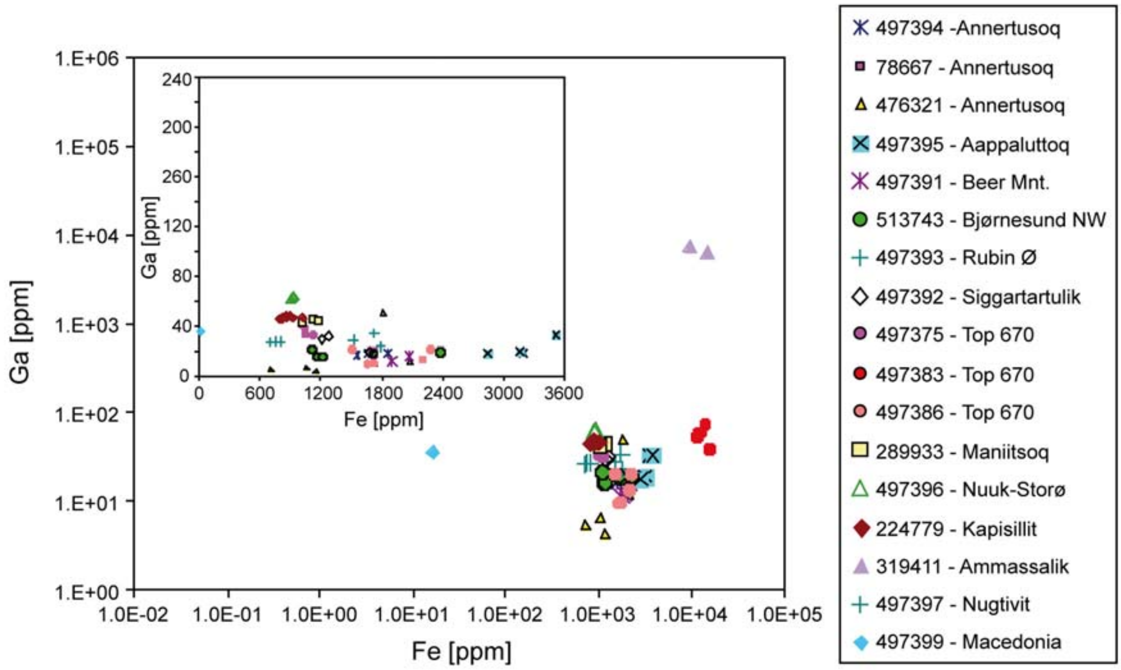

***Figure 27.** Ga vs. Fe diagram for corundum crystals investigated in this study. Inset shows a subset of the data with linear scaling for comparison with. 5 of Thirangoon (inserted).*

The compositional variation in Ga - Fe space is shown in figure 27 (compare with Figure 5 of Thirangoon). The results obtained for corundum from Aappaluttoq obtained by Thirangoon and the results gained from a sample from Aappaluttoq in this study (497395) are in excellent agreement. However, Thirangoon's results that are most likely based on a wide range of crystals from different samples and different sample locations within the Aappaluttoq area show a moderate compositional variation and can be considered as representative for the range of variations that might be expected for a local corundum source. The results obtained in this study for corundum for a variety of Greenlandic sources show an overall much larger variation and are partly overlapping with non-Greenlandic sources (e.g., Thailand, Vietnam, and Afghanistan; cf., figure 5 of Thirangoon). Furthermore, despite a generally narrow within-sample variation, samples from different Greenlandic sources show clear compositional overlaps.

The compositional variation in Ti/V – Fe/Ga and Fe/Ga – V/Cr spaces are shown in figure 28a and 28b), (compare with figures 6 and 7, respectively, of Thirangoon). As for the Ga vs Fe variation, the results obtained for corundum from Aappaluttoq obtained by Thirangoon and in this study are in excellent agreement and Thirangoons results (based on a wide range of crystals from different samples) show a much wider compositional variation (see discussion above).

Again, the results obtained in this study for corundum from a variety of Greenlandic sources show an overall much larger variation than those of Thirangoon and are partly overlapping with non-Greenlandic sources (e.g., Thailand, Vietnam, and Afghanistan; cf., figures 6 and 7 of Thirangoon). Furthermore, despite a generally narrow within-sample variation, corundum samples from different Greenlandic localities show overlapping chemical compositions.

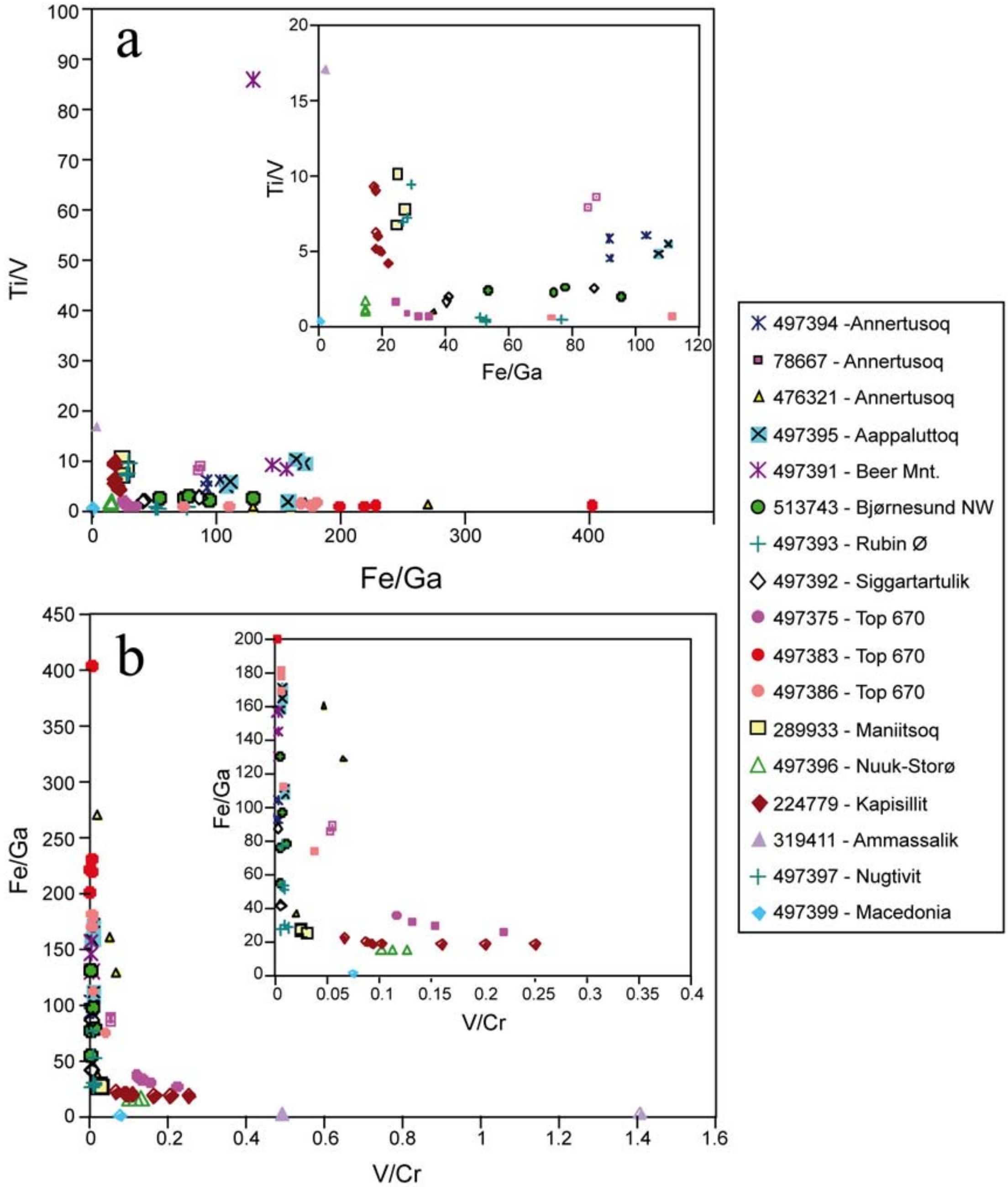

Figure 28. *Ti/V vs. Fe/Ga (a.) and Fe/Ga vs. V/Cr diagrams for corundum crystals investigated in this study. Insets show subsets of the data with blown-up scaling for comparison with figures 5 and 6 of Thirangoon.*

5. Conclusions and recommendations

A total of 16 corundum samples from Greenland (eleven from the Fiskenæsset area, two from the Nuuk area, one from the Maniitsoq area and two from East Greenland) and one sample from Macedonia have been analysed by means of LA-ICP-MS technique, in order to test if geochemical characteristics can be used as a tool for geographical typing of corundum – in particular gemstone qualities like ruby and sapphire. The samples were selected randomly from corundum available among GEUS and BMP staff.

The survey revealed that the samples from Greenland show a relatively homogeneous chemistry and limited intra sample variation.

The results obtained for corundum from Aappaluttoq obtained by Thirangoon and the results gained from a sample from Aappaluttoq in this study are in excellent agreement.

However, the Greenlandic samples plot within relatively continuous fields in the chemical variation diagrams and in the discrimination diagrams that are commonly used to characterise gem corundum. Most significantly, there is an overlap between individual samples that at the present state of knowledge does not allow unequivocal identification of sample provenance based on chemistry alone.

The geochemical signature of the majority of the Greenlandic corundum crystals investigated point to their development in a metamorphic environment closely associated with Mg-rich lithologies.

Three samples (sample 497383 from Top 670, Fiskenæsset; sample 319411 from Tasiilaq and sample 497399 from Macedonia) show distinctive chemical signatures that are related to extreme enrichment or depletion of selected trace elements that allows easy separation of these samples from the bulk of samples investigated. The extreme chemical signatures point to their development in unusual environments. Three samples from Top 670 provide a cautionary tale for geographic typing based on corundum geochemistry alone – even within a single outcrop extreme geochemical variations can occur; in this case it appears to exceed the general variation observed for the entire sample set from Greenland.

This survey shows that the chemistry of some of the Greenlandic corundum samples are partly overlapping with non-Greenlandic sources (e.g., Thailand, Vietnam, and Afghanistan.)

In order to utilise the geochemical record in Greenlandic corundum as a tool for geographical typing, a number of concerted efforts are recommended:

a. Acquisition of a more comprehensive documentation of the geological context of corundum in Greenland.
b. Additional, detailed studies on intra-grain, intra-sample and intra-locality chemical variability of corundum are necessary.
c. Additional crystallographic and optical work, as supplementary data to the geochemical characteristics of corundum.
d. A comprehensive corundum database for comparison purposes. This database should comprise all available information (geological setting and context as well as geochemical, crystallographic and optical parameters) for Greenlandic and non-Greenlandic corundum.
e. All available geochemical, crystallographic and optical parameters obtained on Greenlandic and non-Greenlandic corundum should be used for geographic discrimination employing a multivariate statistical approach, such as pattern recognition with principal component analysis (PCA).

6. Acknowledgement

This project has been initiated on basis of valuable discussions with Henrik Stendal, the Bureau of Minerals and Petroleum (BMP), Greenland. BMP also partly sponsored the project. This support has been highly appreciated.

7. References

Appel, P.W.U. 1995: Ruby occurrences in the Fiskenæsset area, West Greenland. Open File Ser. 95/11, Grønlands geol. Unders. 26 pp

Bøggild, O.B. 1953: The mineralogy of Greenland. Meddr Grønland ,**149**, 3, 442 pp

Calligaro, T., Mossmann, A., Poirot, A. and Querré, J.-P. 1998: Provenance study of rubies from a Parthian statuette by PIXE analysis. Nuclear Instruments & Methods in Physics Research. Section B, Beam Interactions with Materials and Atoms **136–138**, 846–850.

Calligaro, T., Poirot, J.-P. and Querré, G. 1999: Trace element fingerprinting of jewellery rubies by external beam PIXE. Nuclear Instruments and Methods in Physics Research **B150**, 628–634.

Frei, D. and Gerdes, A. 2009: Precise and accurate in-situ U-Pb dating of zircon with high sample throughput by automated LA-SF-ICP-MS. Chemical Geology **261**, 261-270.

Ghisler, M. 1976: The geology, mineralogy and geochemistry of the pre-orogenic Archaean stratiform chromite deposits at Fiskenæsset, West Greenland. In: Borchert, H. (ed.) Monograph Series on Mineral Deposits. **14**, 156 pp. Berlin: Gebr. Borntraeger.

Giesecké, C.L. 1816: The Mineralogical Geology of Greenland; 1816. In: Johnstrup, F.: Gieseckés Mineralogiske Rejse i Grønland. Bianco Lunos Bogtrykkeri, 1878; 372 pp

Gulliong, M. and Günther, D. 2001: Quasi 'non-destructive' laser ablationinductively coupled plasma-mass spectrometry fingerprinting of sapphire. Spectrochimica Acta B **56**, 1219–1231.

Herd, R.K., Windley, B.F. and Ghisler, M. 1969: The mode of occurrence and ptrogenesis of the sapphirine-bearing rocks and associated rocks of West Greenland. Rapp. Grønlands geol. Unders. **24**, 44 pp

Kalsbeek, F. and Garde, A.A. 1989: Geological map of Greenland 1:500 000 Frederiksbhåb Isblink – Søndre Strømfjord Sheet 2 Descriptive text. Copenhagen: Grønlands geol. Unders, 36 pp.

Kornerup, A. and Wanscher, J.H. 1974: Farver i farver. Politikens Forlag, København 1974; 278 pp.

Liebscher, A., Franz, G., Frei, D. and Dulski, P. 2007: High-pressure melting of eclogite and the P-T-X history of tonalitic to trondhjemitic zoisite-pegmatites, Münchberg Massif, Germany. Journal of Petrology **48**, 1001-1019.

Limtrakun, P., Zaw, K., Ryan, C.G. and Mernagh, T.P. 2001: Formation of the Denchai gem sapphires, northern Thailand: evidence from mineral chemistry and fluid/melt inclusion characteristics. Mineralogical Magazine **65**, 725-735.

Myers, J.S. 1985: Stratigraphy and structure of the Fiskenæsset Complex, southern West Greenland. Bull. Grønlands geol. Unders. **150**, 72 pp.

Pearce, N.J., Perkins W.P., Abell, L., Duller, G.A., Fuge, R. 1992: Mineral microanalysis by laser ablation inductively coupled mass spectrometry. Journal of Analytical Atomic Spectrometry **7**, 53-57.

Pearce, N.J.G., Perkins, W.T., Westgate, J.A., Gorton, M.P., Jackson, S.E., Neal, C.R., Chenery, S.P. 1997: A compilation of new and published trace element data for NIST SRM 610 and NIST SRM 612 glass reference material. Geostandards Newsletters **21**, 115-144.

Pedersen, A.K. 1978: Non-stoichiometric magnesian spinels in shale xenoliths from a native iron-bearing andesite at Asuk, Disko, Central West Greenland. Contrib. Mineral. Petrol. ***67***, 331-340, (1978).

Pedersen, A.K. 1981: Armalcolite-bearing Fe-Ti Ocide assemblages in graphite-equilibrated salic volcanic rocks with native iron from Disko, Central West Greenland. Contrib Mineral Petrol ***77***, 307-324, 1981.

Peucat, J.J., Ruffault, P., Fritsch, E., Bouhnik-Le, C., Simonet, C. and Lasnier, B. 2007: Ga/Mg ratio as a new geochemical tool to differentiate magmatic from metamorphic blue sapphires. Lithos **98**, 261-274.

Saminpanya, S., Manning, D. and Henderson, D. 2003: Trace elements in Thai gem corundums. Journal of Gemmology **28**, 392–398.

Sutherland, F.L. & Abduriyim, A. 2009: Geographic typing of gem corundum: A test case for Australia. Journal of Gemmology 31 (5-8), 203-210.

Sutherland, F.L., Hoskin, P.W.O., Fanning, C.M., and Coenraads, R.R. 1998: Models of corundum origin from alkali basalt terrains: a reappraisal. Contributions to Mineralogy and Petrology **133**, 356–372

Thirangoon, K. 2009: Ruby and pink sapphire from Aappaluttoq, Greenland. Status of on-going research. Internal confidential report, received from BMP.

Weston, B. 2009: 2008 Report on Field Activities for the Fiskenæsset Ruby Project, Greenland. Internal Company Report, available from the True North Gems website.

Appendix

Table2. Analytical results for rubies investigated in this study.							
Region	**Locality**	**Sample**	**Mg**	**Si**	**Ti**	**V**	**Cr**
Fiskenæsset	**Angertussoq**	**497394**	63.67	1196.35	39.01	8.62	6504.56
		497394	71.22	1122.05	40.89	7.04	3558.98
		497394	68.34	1165.82	63.16	10.57	5921.02
Fiskenæsset	**Angertussoq**	**78667**	45.05	1207.09	120.41	15.22	287.23
		78667	51.71	1042.75	144.75	16.82	307.80
Fiskenæsset	**Annertusoq**	**476321**	61.78	1087.76	54.86	99.90	1545.53
		476321	68.71	1003.26	56.18	125.78	2738.18
		476321	35.13	1316.99	63.87	63.94	3357.46
		476321	616.71	3621.34	34.94	20.33	3289.00
		476321	85.16	1124.88	97.14	88.59	4867.99
Fiskenæsset	**Aappaluttoq**	**497395**	45.70	1136.93	265.29	28.70	4977.37
		497395	46.94	1068.09	277.28	27.94	5213.15
		497395	29.91	1111.80	34.78	22.68	6061.15
		497395	46.49	1169.60	272.86	56.48	6583.56
		497395	74.64	1133.75	337.83	62.03	7445.39
Fiskenæsset	**Beer Mt.**	**497391**	40.47	1019.63	35.30	4.37	3580.33
		497391	41.50	1046.22	33.49	3.80	2516.06
		497391	87.47	1005.26	613.04	7.12	3776.20
Fiskenæsset	**Bjørnesund NW**	**513743**	45.85	1128.94	36.03	16.83	4157.83
		513743	53.57	1119.67	32.37	12.77	1228.54
		513743	56.40	1152.90	37.67	16.08	4258.49
		513743	49.94	1142.43	30.79	16.43	3044.57
		513743	46.09	1077.10	28.65	12.30	2819.14
Fiskenæsset	**Rubin Ø**	**497393**	25.89	1025.85	22.00	73.77	11429.87
		497393	41.22	1057.82	26.04	58.99	9299.48
		497393	33.87	1003.73	25.92	69.57	9124.94
		497393	43.38	1032.72	47.14	86.89	11085.91
Fiskenæsset	**Siggartartulik**	**497392**	52.46	1005.21	41.26	25.88	5520.03
		497392	53.82	993.05	44.22	23.63	4951.22
		497392	43.97	1060.11	33.98	13.36	6050.14
Fiskenæsset	**Top 670**	**497375**	74.23	1114.14	100.53	65.02	294.82
		497375	251.59	1246.75	49.83	59.41	386.77
		497375	42.48	1190.74	33.02	53.14	403.75
		497375	56.04	1161.13	39.00	59.17	506.32
Fiskenæsset	**Top 670**	**497383**	342656.50	88984.43	62.89	86.81	24508.75
		497383	343990.19	88286.96	57.20	100.18	69433.90
		497383	346947.91	90226.45	82.15	119.95	31026.43
		497383	415215.66	126328.90	92.88	104.81	45438.80
		497383	381952.38	100094.43	59.11	86.86	61062.46
Fiskenæsset	**Top 670**	**497386**	31.72	1199.26	18.93	20.31	3517.88
		497386	33.09	1106.15	14.72	24.32	3558.13
		497386	41.10	1153.94	27.54	20.54	3847.83
		497386	53.19	1107.29	24.47	45.06	1185.80
		497386	56.18	1127.72	31.06	27.03	5094.94
Maniitsoq	**Maniitsoq**	**289933**	134.31	1004.39	708.81	70.14	2904.24
		289933	111.51	1004.25	550.32	71.31	3033.40
		289933	82.11	997.33	457.08	68.25	2301.42
Nuuk	**Nuuk - Storø**	**497396**	64.84	1078.33	100.58	96.19	852.71
		497396	64.29	1130.26	151.34	88.85	878.42
		497396	66.21	1130.76	96.26	84.36	664.36
Nuuk	**Kapisillit**	**224779**	168.76	971.86	767.47	82.23	327.67
		224779-1	118.62	975.32	450.83	87.22	544.67
		224779-1	131.26	969.81	535.13	86.10	845.76
		224779-2	173.16	948.13	790.56	87.71	433.05
		224779-2	141.73	1006.94	540.66	90.43	973.72
		224779-2	113.97	996.58	430.79	86.41	988.23
		224779-2	102.50	1006.78	373.80	88.67	1351.40

Table2. Analytical results for rubies investigated in this study.							
Region	**Locality**	**Sample**	**Mg**	**Si**	**Ti**	**V**	**Cr**
East Greenland	**Tasiilaq**	**319411**	5964.65	559042.44	1095.28	64.04	45.46
		319411	4923.49	545935.00	929.09	20.53	41.94
East Greenland	**Nugtivit**	**497397**	9.23	1150.46	29.20	4.22	951.63
		497397	18.88	1136.89	35.66	4.92	424.65
		497397	23.90	1262.69	43.74	4.64	550.00
International	**Macedonia**	**497399**	23.93	1048.59	13.72	41.15	551.27
		497399	10.40	1119.46	24.13	37.87	366.52
		497399	10.96	964.61	20.58	36.43	370.64

Table2. Analytical results for rubies investigated in this stu							
Region	**Locality**	**Sample**	**Fe**	**Ga**	**Fe+Ti**	**Cr/Ga**	**Ga/Mg**
Fiskenæsset	**Angertussoq**	**497394**	1557.39	16.87	1596.4	385.57	0.26
		497394	1671.26	18.19	1712.15	195.66	0.26
		497394	1853.76	17.88	1916.92	331.15	0.26
Fiskenæsset	**Angertussoq**	**78667**	1683.16	19.75	1803.57	14.54	0.44
		78667	1738.60	19.77	1883.35	15.57	0.38
Fiskenæsset	**Annertusoq**	**476321**	709.71	5.51	764.57	280.50	0.09
		476321	1058.28	6.62	1114.46	413.62	0.10
		476321	1818.77	50.09	1882.64	67.03	1.43
		476321	2076.57	12.13	2111.51	271.15	0.02
		476321	1148.86	4.26	1246	1142.72	0.05
Fiskenæsset	**Aappaluttoq**	**497395**	3185.49	18.63	3450.78	267.17	0.41
		497395	3163.95	19.24	3441.23	270.95	0.41
		497395	2844.85	18.03	2879.63	336.17	0.60
		497395	3519.15	32.75	3792.01	201.02	0.70
		497395	3722.14	33.59	4059.97	221.65	0.45
Fiskenæsset	**Beer Mt.**	**497391**	1896.50	12.10	1931.8	295.90	0.30
		497391	1715.90	11.82	1749.39	212.86	0.28
		497391	2071.07	15.96	2684.11	236.60	0.18
Fiskenæsset	**Bjørnesund NW**	**513743**	1168.98	15.68	1205.01	265.17	0.34
		513743	1224.17	15.67	1256.54	78.40	0.29
		513743	1118.08	20.86	1155.75	204.15	0.37
		513743	1717.50	17.94	1748.29	169.71	0.36
		513743	2385.64	18.43	2414.29	152.96	0.40
Fiskenæsset	**Rubin Ø**	**497393**	1522.50	28.86	1544.5	396.05	1.11
		497393	1792.56	23.32	1818.6	398.78	0.57
		497393	1529.40	28.82	1555.32	316.62	0.85
		497393	1729.23	34.06	1776.37	325.48	0.79
Fiskenæsset	**Siggartartulik**	**497392**	1272.74	31.56	1314	174.91	0.60
		497392	1207.75	29.31	1251.97	168.93	0.54
		497392	1679.08	19.33	1713.06	312.99	0.44
Fiskenæsset	**Top 670**	**497375**	1010.18	41.02	1110.71	7.19	0.55
		497375	1052.66	37.40	1102.49	10.34	0.15
		497375	1044.63	32.91	1077.65	12.27	0.77
		497375	1123.28	32.27	1162.28	15.69	0.58
Fiskenæsset	**Top 670**	**497383**	11920.34	51.95	11983.23	471.78	0.00015
		497383	12793.05	58.14	12850.25	1194.25	0.00017
		497383	12368.58	56.58	12450.73	548.36	0.00016
		497383	15742.50	39.00	15835.38	1165.10	0.00009
		497383	14126.79	70.75	14185.9	863.07	0.00019
Fiskenæsset	**Top 670**	**497386**	1726.17	9.73	1745.1	361.55	0.31
		497386	2288.22	20.48	2302.94	173.74	0.62
		497386	1658.34	9.19	1685.88	418.70	0.22
		497386	1513.92	20.51	1538.39	57.82	0.39
		497386	2213.57	13.13	2244.63	388.04	0.23
Maniitsoq	**Maniitsoq**	**289933**	1123.49	44.80	1832.3	64.83	0.33
		289933	1178.32	43.27	1728.64	70.10	0.39
		289933	1027.90	41.99	1484.98	54.81	0.51
Nuuk	**Nuuk - Storø**	**497396**	935.08	64.02	1035.66	13.32	0.99
		497396	903.33	62.48	1054.67	14.06	0.97
		497396	926.23	63.41	1022.49	10.48	0.96
Nuuk	**Kapisillit**	**224779**	798.80	45.56	1566.27	7.19	0.27
		224779-1	824.06	46.11	1274.89	11.81	0.39
		224779-1	852.98	46.59	1388.11	18.15	0.35
		224779-2	855.91	47.73	1646.47	9.07	0.28
		224779-2	892.57	48.39	1433.23	20.12	0.34
		224779-2	920.24	46.81	1351.03	21.11	0.41
		224779-2	1020.96	46.97	1394.76	28.77	0.46

Table2. Analytical results for rubies investigated in this stu							
Region	**Locality**	**Sample**	**Fe**	**Ga**	**Fe+Ti**	**Cr/Ga**	**Ga/Mg**
East Greenland	**Tasiilaq**	**319411**	14756.75	6572.33	15852.03	0.01	1.10
		319411	9421.28	7593.65	10350.37	0.01	1.54
East Greenland	**Nugtivit**	**497397**	709.61	26.85	738.81	35.44	2.91
		497397	755.53	27.29	791.19	15.56	1.45
		497397	807.48	27.54	851.22	19.97	1.15
International	**Macedonia**	**497399**	16.38	35.23	30.1	15.65	1.47
		497399		33.21	24.13	11.04	3.19
		497399		32.35	20.58	11.46	2.95

Table2. Analytical results for rubies investigated in this stu							
Region	**Locality**	**Sample**	**Fe/Ti**	**Fe/Mg**	**Fe**	**Fe/Ti**	**Cr/Ga**
Fiskenæsset	**Angertussoq**	**497394**	39.9	24.460	1557.39	39.9	385.57
		497394	40.9	23.466	1671.26	40.9	195.66
		497394	29.4	27.126	1853.76	29.4	331.15
Fiskenæsset	**Angertussoq**	**78667**	14.0	37.362	1683.16	14.0	14.54
		78667	12.0	33.622	1738.6	12.0	15.57
Fiskenæsset	**Annertusoq**	**476321**	12.9	11.488	709.71	12.9	280.50
		476321	18.8	15.402	1058.28	18.8	413.62
		476321	28.5	51.773	1818.77	28.5	67.03
		476321	59.4	3.367	2076.57	59.4	271.15
		476321	11.8	13.491	1148.86	11.8	1142.72
Fiskenæsset	**Aappaluttoq**	**497395**	12.0	69.704	3185.49	12.0	267.17
		497395	11.4	67.404	3163.95	11.4	270.95
		497395	81.8	95.114	2844.85	81.8	336.17
		497395	12.9	75.697	3519.15	12.9	201.02
		497395	11.0	49.868	3722.14	11.0	221.65
Fiskenæsset	**Beer Mt.**	**497391**	53.7	46.862	1896.5	53.7	295.90
		497391	51.2	41.347	1715.9	51.2	212.86
		497391	3.4	23.677	2071.07	3.4	236.60
Fiskenæsset	**Bjørnesund NW**	**513743**	32.4	25.496	1168.98	32.4	265.17
		513743	37.8	22.852	1224.17	37.8	78.40
		513743	29.7	19.824	1118.08	29.7	204.15
		513743	55.8	34.391	1717.5	55.8	169.71
		513743	83.3	51.760	2385.64	83.3	152.96
Fiskenæsset	**Rubin Ø**	**497393**	69.2	58.806	1522.5	69.2	396.05
		497393	68.8	43.488	1792.56	68.8	398.78
		497393	59.0	45.155	1529.4	59.0	316.62
		497393	36.7	39.862	1729.23	36.7	325.48
Fiskenæsset	**Siggartartulik**	**497392**	30.8	24.261	1272.74	30.8	174.91
		497392	27.3	22.441	1207.75	27.3	168.93
		497392	49.4	38.187	1679.08	49.4	312.99
Fiskenæsset	**Top 670**	**497375**	10.0	13.609	1010.18	10.0	7.19
		497375	21.1	4.184	1052.66	21.1	10.34
		497375	31.6	24.591	1044.63	31.6	12.27
		497375	28.8	20.044	1123.28	28.8	15.69
Fiskenæsset	**Top 670**	**497383**	189.5	0.035	11920.34	189.5	471.78
		497383	223.7	0.037	12793.05	223.7	1194.25
		497383	150.6	0.036	12368.58	150.6	548.36
		497383	169.5	0.038	15742.5	169.5	1165.10
		497383	239.0	0.037	14126.79	239.0	863.07
Fiskenæsset	**Top 670**	**497386**	91.2	54.419	1726.17	91.2	361.55
		497386	155.4	69.151	2288.22	155.4	173.74
		497386	60.2	40.349	1658.34	60.2	418.70
		497386	61.9	28.462	1513.92	61.9	57.82
		497386	71.3	39.401	2213.57	71.3	388.04
Maniitsoq	**Maniitsoq**	**289933**	1.6	8.365	1123.49	1.6	64.83
		289933	2.1	10.567	1178.32	2.1	70.10
		289933	2.2	12.519	1027.9	2.2	54.81
Nuuk	**Nuuk - Storø**	**497396**	9.3	14.421	935.08	9.3	13.32
		497396	6.0	14.051	903.33	6.0	14.06
		497396	9.6	13.989	926.23	9.6	10.48
Nuuk	**Kapisillit**	**224779**	1.0	4.733	798.8	1.0	7.19
		224779-1	1.8	6.947	824.06	1.8	11.81
		224779-1	1.6	6.498	852.98	1.6	18.15
		224779-2	1.1	4.943	855.91	1.1	9.07
		224779-2	1.7	6.298	892.57	1.7	20.12
		224779-2	2.1	8.074	920.24	2.1	21.11
		224779-2	2.7	9.961	1020.96	2.7	28.77

Table2. Analytical results for rubies investigated in this stu							
Region	**Locality**	**Sample**	**Fe/Ti**	**Fe/Mg**	**Fe**	**Fe/Ti**	**Cr/Ga**
East Greenland	**Tasiilaq**	**319411**	13.5	2.474	14756.75	13.5	0.01
		319411	10.1	1.914	9421.28	10.1	0.01
East Greenland	**Nugtivit**	**497397**	24.3	76.881	709.61	24.3	35.44
		497397	21.2	40.017	755.53	21.2	15.56
		497397	18.5	33.786	807.48	18.5	19.97
International	**Macedonia**	**497399**	1.2	0.684	16.38	1.2	15.65
		497399					
		497399					

Table2. Analytical results for rubies investigated in this stu							
Region	**Locality**	**Sample**	**TiO2**	**V2O5**	**Cr2O3**	**Fe2O3**	**Ga2O3**
Fiskenæsset	**Angertussoq**	**497394**	65.07	15.39	9503.16	2227.07	22.67
		497394	68.20	12.57	5199.67	2389.90	24.45
		497394	105.35	18.87	8650.61	2650.88	24.03
Fiskenæsset	**Angertussoq**	**78667**	200.84	27.17	419.64	2406.92	26.54
		78667	241.44	30.02	449.70	2486.20	26.57
Fiskenæsset	**Annertusoq**	**476321**	91.51	178.32	2258.02	1014.89	7.41
		476321	93.71	224.52	4000.48	1513.34	8.90
		476321	106.54	114.13	4905.25	2600.84	67.32
		476321	58.28	36.29	4805.23	2969.50	16.30
		476321	162.03	158.13	7112.13	1642.87	5.73
Fiskenæsset	**Aappaluttoq**	**497395**	442.50	51.23	7271.94	4555.25	25.04
		497395	462.50	49.87	7616.41	4524.45	25.86
		497395	58.01	40.48	8855.34	4068.14	24.23
		497395	455.13	100.82	9618.58	5032.38	44.02
		497395	563.50	110.72	10877.71	5322.66	45.14
Fiskenæsset	**Beer Mt.**	**497391**	58.88	7.80	5230.86	2712.00	16.26
		497391	55.86	6.78	3675.96	2453.74	15.89
		497391	1022.55	12.71	5517.03	2961.63	21.45
Fiskenæsset	**Bjørnesund NW**	**513743**	60.10	30.04	6074.59	1671.64	21.07
		513743	53.99	22.79	1794.90	1750.56	21.06
		513743	62.83	28.70	6221.65	1598.85	28.04
		513743	51.36	29.33	4448.12	2456.03	24.11
		513743	47.79	21.96	4118.76	3411.47	24.77
Fiskenæsset	**Rubin Ø**	**497393**	36.70	131.68	16699.04	2177.18	38.79
		497393	43.43	105.30	13586.54	2563.36	31.34
		497393	43.23	124.18	13331.54	2187.04	38.73
		497393	78.63	155.10	16196.51	2472.80	45.78
Fiskenæsset	**Siggartartulik**	**497392**	68.82	46.20	8064.76	1820.02	42.42
		497392	73.76	42.18	7233.73	1727.08	39.39
		497392	56.68	23.85	8839.25	2401.08	25.98
Fiskenæsset	**Top 670**	**497375**	167.68	116.06	430.73	1444.56	55.13
		497375	83.12	106.05	565.07	1505.30	50.27
		497375	55.08	94.85	589.88	1493.82	44.23
		497375	65.05	105.62	739.73	1606.29	43.37
Fiskenæsset	**Top 670**	**497383**	104.90	154.96	35807.28	17046.09	69.82
		497383	95.41	178.82	101442.93	18294.06	78.14
		497383	137.03	214.11	45329.61	17687.07	76.04
		497383	154.92	187.09	66386.09	22511.78	52.42
		497383	98.60	155.05	89212.25	20201.31	95.09
Fiskenæsset	**Top 670**	**497386**	31.58	36.25	5139.62	2468.42	13.08
		497386	24.55	43.41	5198.43	3272.15	27.53
		497386	45.94	36.66	5621.68	2371.43	12.35
		497386	40.82	80.43	1732.45	2164.91	27.57
		497386	51.81	48.25	7443.71	3165.41	17.65
Maniitsoq	**Maniitsoq**	**289933**	1182.30	125.20	4243.09	1606.59	60.21
		289933	917.93	127.29	4431.80	1685.00	58.15
		289933	762.41	121.83	3362.37	1469.90	56.43
Nuuk	**Nuuk - Storø**	**497396**	167.77	171.70	1245.81	1337.16	86.04
		497396	252.44	158.60	1283.37	1291.76	83.97
		497396	160.56	150.58	970.63	1324.51	85.22
Nuuk	**Kapisillit**	**224779**	1280.14	146.78	478.73	1142.28	61.23
		224779-1	751.98	155.69	795.76	1178.41	61.97
		224779-1	892.60	153.69	1235.66	1219.76	62.62
		224779-2	1318.65	156.56	632.69	1223.95	64.15
		224779-2	901.82	161.42	1422.60	1276.38	65.04
		224779-2	718.56	154.24	1443.80	1315.94	62.91
		224779-2	623.50	158.28	1974.40	1459.97	63.13

Table2. Analytical results for rubies investigated in this stu							
Region	**Locality**	**Sample**	**TiO2**	**V2O5**	**Cr2O3**	**Fe2O3**	**Ga2O3**
East Greenland	**Tasiilaq**	**319411**	1826.93	114.31	66.42	21102.15	8833.21
		319411	1549.72	36.65	61.27	13472.43	10205.87
East Greenland	**Nugtivit**	**497397**	48.71	7.53	1390.33	1014.74	36.09
		497397	59.48	8.78	620.41	1080.41	36.68
		497397	72.96	8.28	803.55	1154.70	37.01
International	**Macedonia**	**497399**	22.88	73.45	805.41	23.42	47.35
		497399	40.25	67.60	535.49		44.63
		497399	34.33	65.03	541.51		43.48

Table2. Analytical results for rubies investigated in this stu						
Region	**Locality**	**Sample**	**Fe2O3/TiO2**	**Cr2O3/Ga2(**	**Fe2O3/Cr2(**	**TiO2/Ga2O3**
Fiskenæsset	**Angertussoq**	**497394**	34.226	419.135	0.234	2.870
		497394	35.040	212.688	0.460	2.790
		497394	25.162	359.981	0.306	4.384
Fiskenæsset	**Angertussoq**	**78667**	11.984	15.809	5.736	7.566
		78667	10.297	16.924	5.529	9.087
Fiskenæsset	**Annertusoq**	**476321**	11.091	304.914	0.449	12.357
		476321	16.149	449.630	0.378	10.532
		476321	24.413	72.864	0.530	1.582
		476321	50.952	294.750	0.618	3.575
		476321	10.139	1242.199	0.231	28.300
Fiskenæsset	**Aappaluttoq**	**497395**	10.294	290.428	0.626	17.673
		497395	9.783	294.541	0.594	17.886
		497395	70.125	365.435	0.459	2.394
		497395	11.057	218.525	0.523	10.340
		497395	9.446	240.951	0.489	12.482
Fiskenæsset	**Beer Mt.**	**497391**	46.059	321.654	0.518	3.621
		497391	43.926	231.395	0.668	3.516
		497391	2.896	257.201	0.537	47.671
Fiskenæsset	**Bjørnesund NW**	**513743**	27.815	288.252	0.275	2.852
		513743	32.422	85.226	0.975	2.564
		513743	25.446	221.918	0.257	2.241
		513743	47.822	184.482	0.552	2.130
		513743	71.387	166.281	0.828	1.929
Fiskenæsset	**Rubin Ø**	**497393**	59.330	430.523	0.130	0.946
		497393	59.016	433.492	0.189	1.386
		497393	50.586	344.181	0.164	1.116
		497393	31.449	353.816	0.153	1.718
Fiskenæsset	**Siggartartulik**	**497392**	26.445	190.132	0.226	1.623
		497392	23.415	183.632	0.239	1.872
		497392	42.363	340.239	0.272	2.182
Fiskenæsset	**Top 670**	**497375**	8.615	7.813	3.354	3.042
		497375	18.111	11.242	2.664	1.654
		497375	27.122	13.336	2.532	1.245
		497375	24.692	17.056	2.171	1.500
Fiskenæsset	**Top 670**	**497383**	162.498	512.846	0.476	1.502
		497383	191.742	1298.218	0.180	1.221
		497383	129.078	596.101	0.390	1.802
		497383	145.309	1266.523	0.339	2.956
		497383	204.891	938.207	0.226	1.037
Fiskenæsset	**Top 670**	**497386**	78.176	393.024	0.480	2.415
		497386	133.269	188.861	0.629	0.892
		497386	51.624	455.147	0.422	3.719
		497386	53.041	62.849	1.250	1.481
		497386	61.099	421.818	0.425	2.936
Maniitsoq	**Maniitsoq**	**289933**	1.359	70.470	0.379	19.636
		289933	1.836	76.207	0.380	15.784
		289933	1.928	59.580	0.437	13.510
Nuuk	**Nuuk - Storø**	**497396**	7.970	14.479	1.073	1.950
		497396	5.117	15.283	1.007	3.006
		497396	8.249	11.389	1.365	1.884
Nuuk	**Kapisillit**	**224779**	0.892	7.818	2.386	20.906
		224779-1	1.567	12.841	1.481	12.134
		224779-1	1.367	19.734	0.987	14.255
		224779-2	0.928	9.863	1.935	20.556
		224779-2	1.415	21.874	0.897	13.866
		224779-2	1.831	22.949	0.911	11.422
		224779-2	2.342	31.276	0.739	9.877

Table2. Analytical results for rubies investigated in this stu						
Region	**Locality**	**Sample**	**Fe2O3/TiO2**	**Cr2O3/Ga2(**	**Fe2O3/Cr2(**	**TiO2/Ga2O3**
East Greenland	**Tasiilaq**	**319411**	11.551	0.008	317.722	0.207
		319411	8.693	0.006	219.871	0.152
East Greenland	**Nugtivit**	**497397**	20.834	38.528	0.730	1.350
		497397	18.164	16.915	1.741	1.622
		497397	15.827	21.709	1.437	1.971
International	**Macedonia**	**497399**	1.024	17.010	0.029	0.483
		497399		11.997		0.902
		497399		12.455		0.790

78667

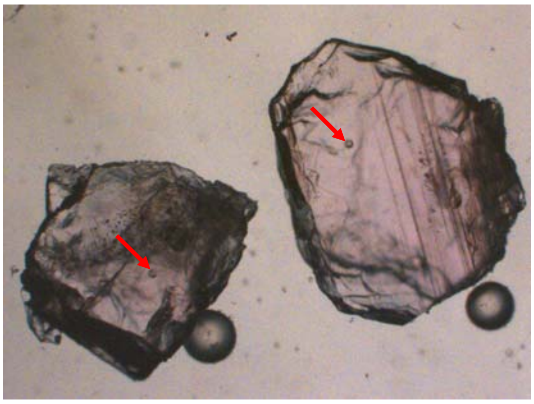

78667

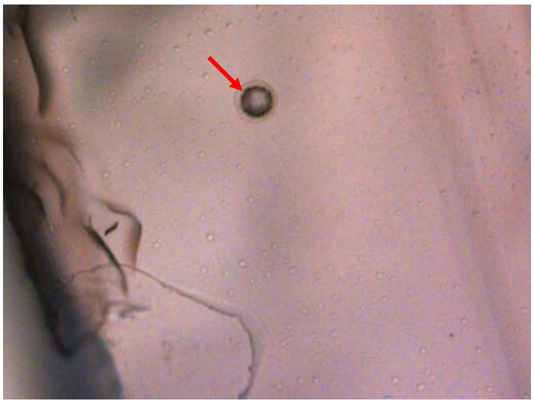

476321

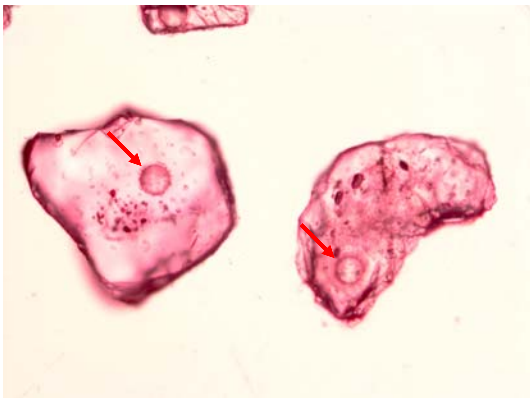

476321

497394

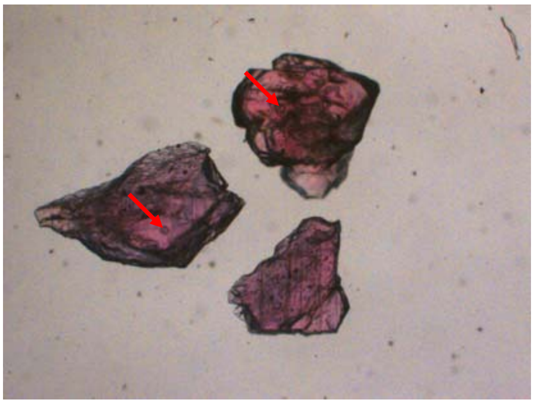

497394

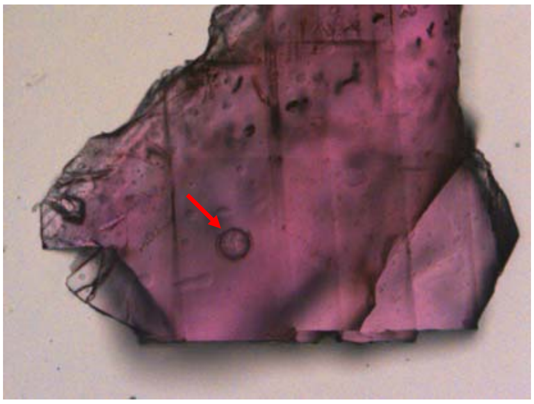

497392

497392

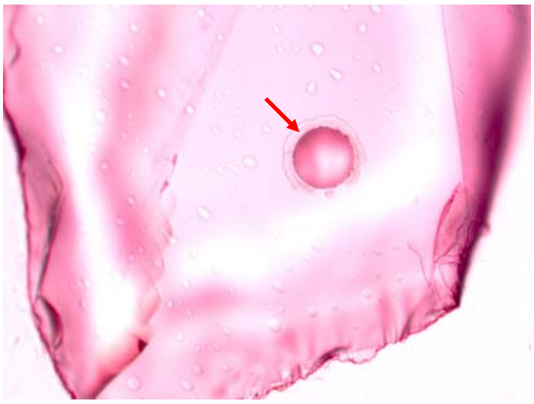

497395

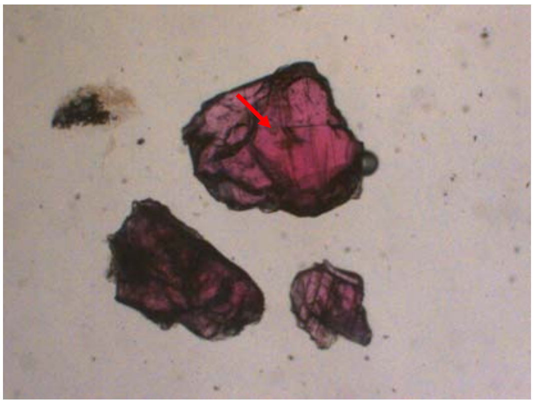

497395

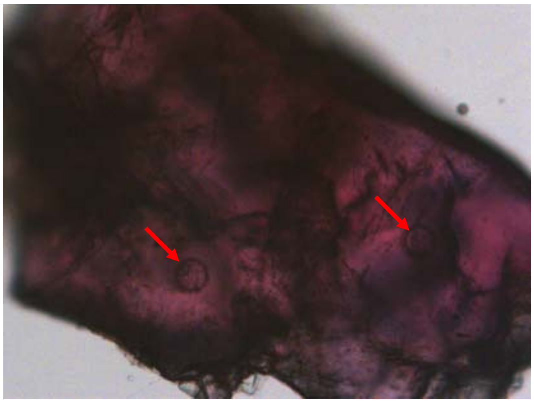

497391

497391

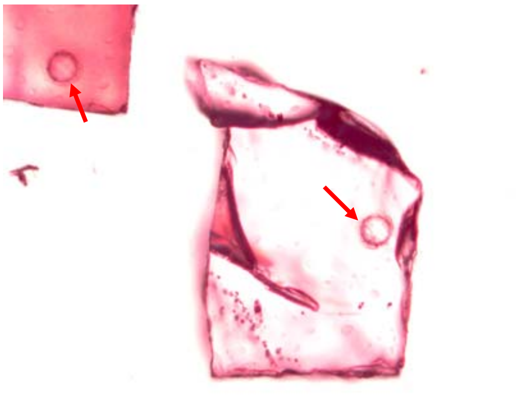

513733 or 743?

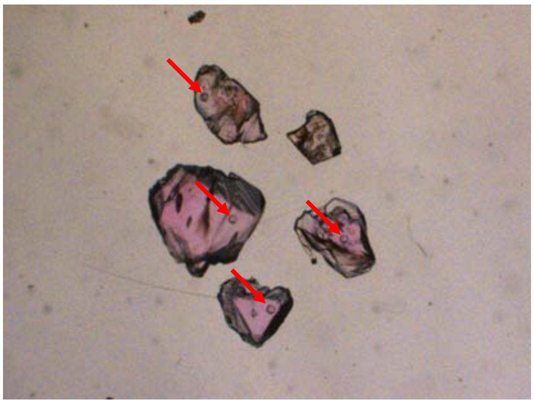

513733 or 743?

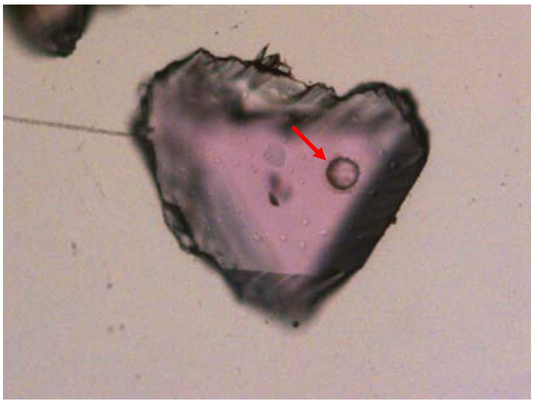

497393

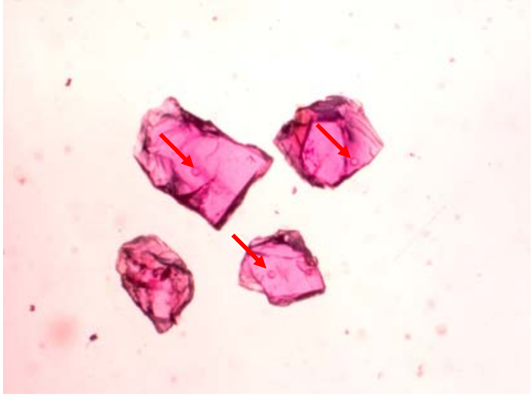

497393

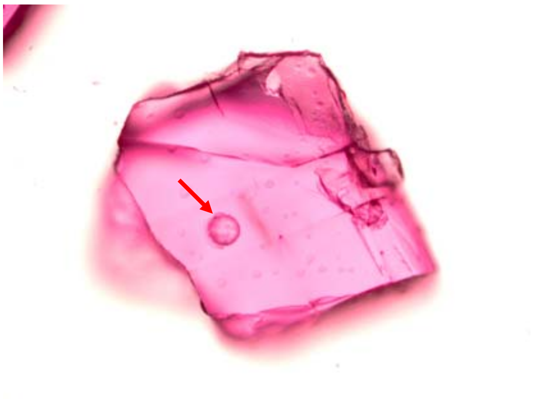

497375

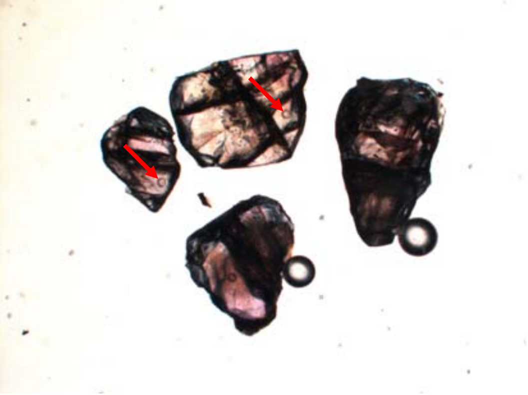

497375

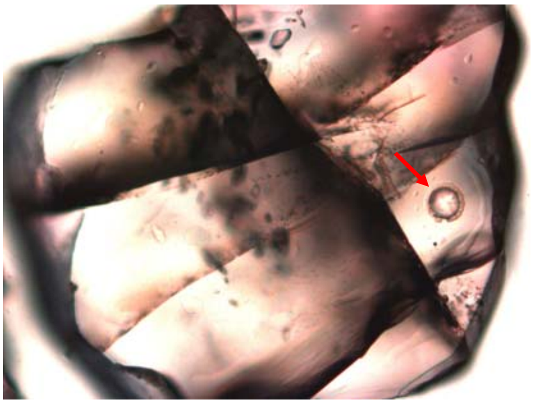

497375

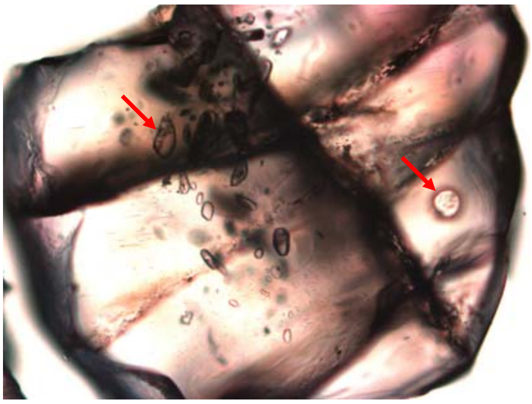

497383

497383

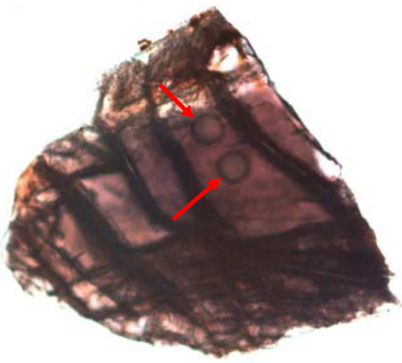

224779

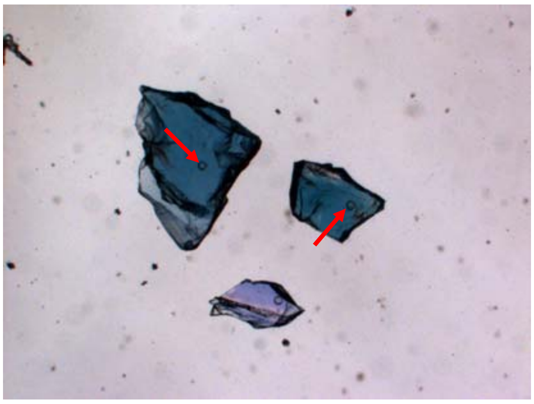

224779

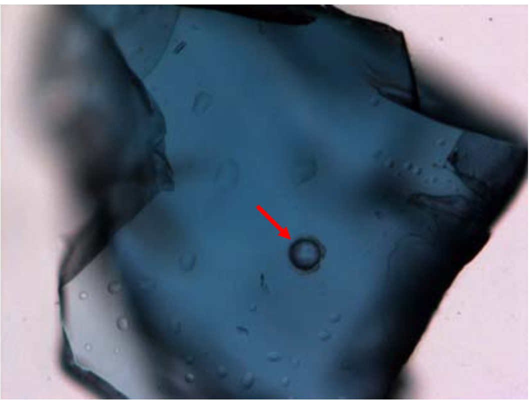

497396

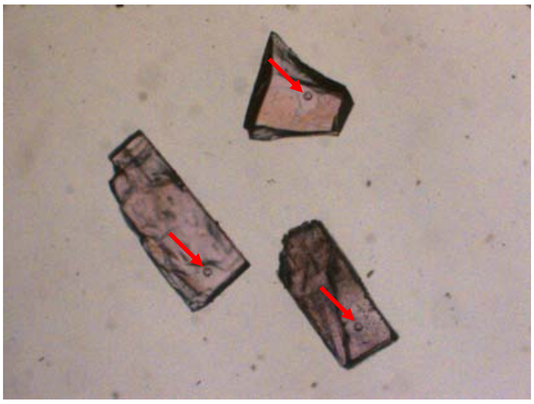

497396

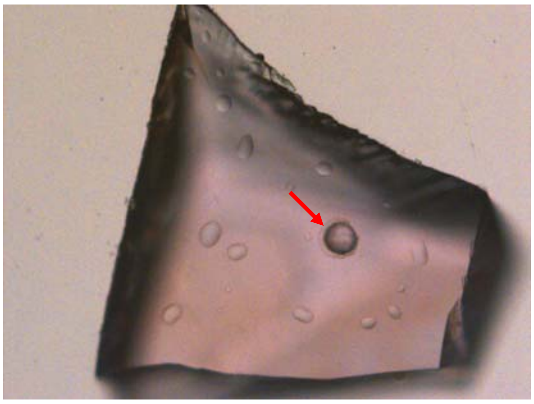

289933

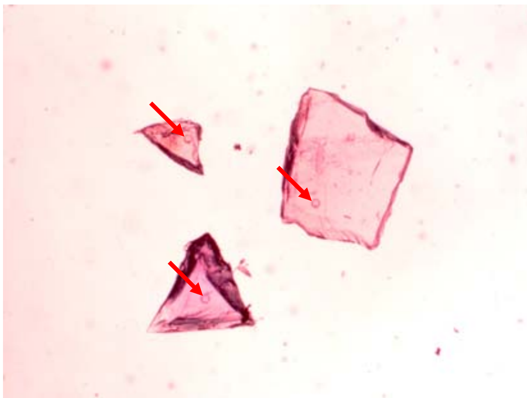

289933

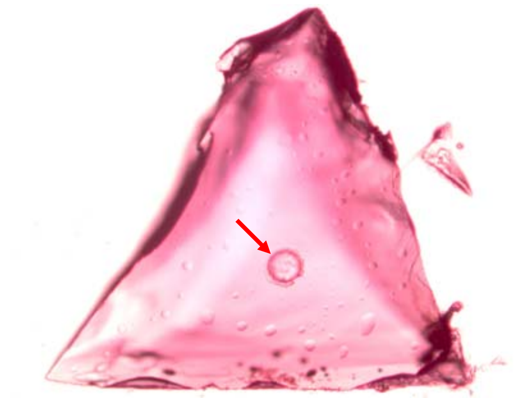

497397

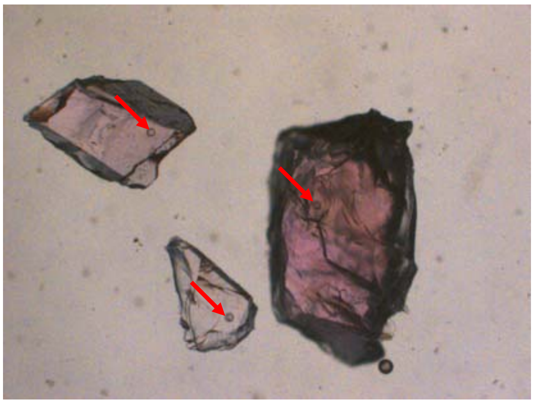

497397

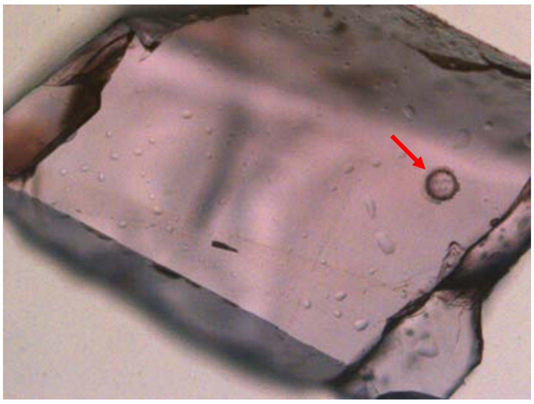

319411

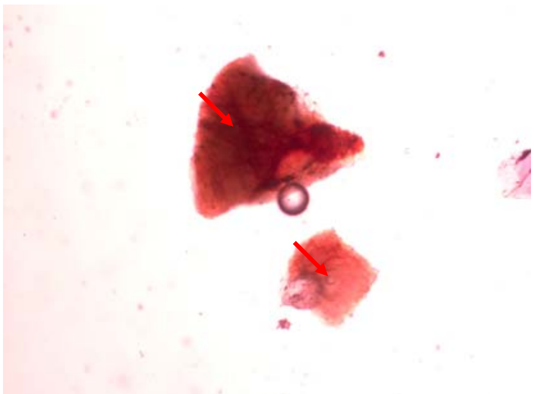

319411

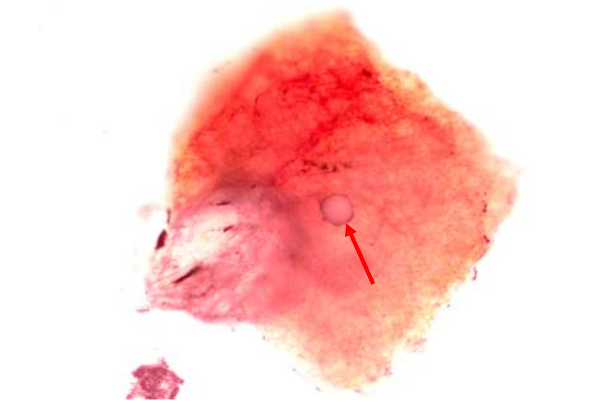

497399

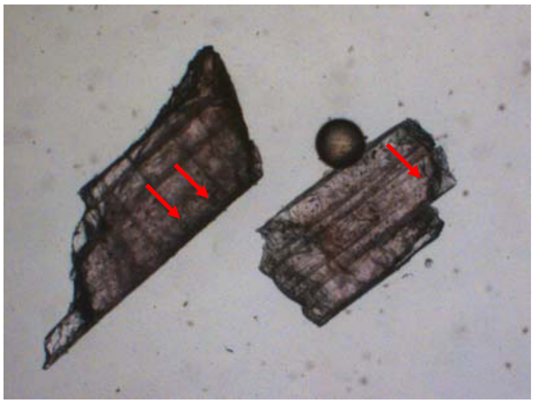

497399